VERTICAL ASSESSMENT OF FUSED DEM FROM ASTER-1″, COPERNICUS-1″, NASADEM-1″ & SRTM-1″-v3 PUBLIC GDEMs USING GPS GROUND CONTROLS IN TANZANIA.

SULEIMAN, SULEIMAN H

A Dissertation Submitted to the Department of Geospatial Sciences and Technology in Partially Fulfilment of the Requirements for the Award of Science in Geomatics (BSc. GM) of Ardhi University

CERTIFICATION

The undersigned certify that they have proof read and hereby recommend for acceptance by the Ardhi University a dissertation titled "**Vertical Assessment of Fused DEM from ASTER-1″, COPERNICUS-1″, NASADEM-1″ & SRTM-1″-v3 Public GDEMs Using GPS Ground Controls in Tanzania**", in partial fulfillment of the requirements for the award of degree of Bachelor of Science in Geomatics at Ardhi University.

……..

MS. REGINA V. PETER

(Supervisor)

Date.....

DECLARATION AND COPYRIGHT

I, SULEIMAN, SULEIMAN H hereby declare that, the contents of this dissertation are the results of my own findings through my study and investigation, and to the best of my knowledge, they have not been presented anywhere else as a dissertation for diploma, degree or any similar academic award in any institution of higher learning.

……..

SULEIMAN, SULEIMAN H

22827/T.2019

(Candidate)

ACKNOWLEDGEMENT

The completion of this research could not have been possible without the participation, support and assistance of many people whose names may not all be enumerated. Their contribution is sincerely appreciated and gratefully acknowledged.

First and foremost, I would like to thank the Almighty GOD who gave me strength, patience and good health which helped in the completion of this research.

Second, I am very grateful to my research supervisors Ms. Regina V. Peter for her assistance on my research topic. Also, her constant supervision in checking and correcting the research report, clarification in all challenges, contradictions from the research topic and sharing her best knowledge in all matters regarding the research is a remarkable contribution to this research.

Also I would like to thank Department of Geospatial Science and Technology (DGST), for their contributions during intermediate presentation sessions which helped me in one way or another to successfully complete this research.

Mom and Dad, your love, support and wisdom are the reason I am where I am today. You are both wonderful people and I feel very blessed that you are my parents. Thank you for encouraging me to follow my interests, and for instilling in me an appreciation for discovery and learning. Thank you, most of all, for teaching me to have a good sense of humour and to laugh when possible at the inevitable ups and downs of life.

Lastly but not least, I like to thank my colleagues, fourth year students 2019/2023 Department of Geospatial Sciences and Technology (DGST) for their cooperation during my four years of study and to all who in one way or another have helped and encouraged me during this research. .

DEDICATION

I dedicate this dissertation to my father Haji Suleiman, my mother Kaima Omar, my brother Omar Haji, my sisters Salama Haji, Aisha Haji, and Najat Haji, my uncle Mzee Omar and my Colleagues (Geomatics and Geoinformatics year 2019-2023) through their patience, understanding, prayers, love, support and encourage on my academic journey.

ABSTRACT

Digital Elevation Models (DEMs) are usually generated from different sensors and processing techniques. Due to the sensor's technologies, the variations in DEMs accuracy are obvious. DEMs fusion techniques are one of the solutions of reducing DEM errors. The crucial technical problematic of DEM fusion is that it requires weights to quantify the effect of the inputs DEM. These weights are a function of the height accuracy, and typically vary significantly across each DEM, due to the sensor technology, scene characteristics and method used to generate it. This study reviewed the vertical assessment of fused DEM from COPERNICUS-1″, NASADEM-1″, SRTM-1″ and ASTER-1″ Public GDEM using GPS Ground Control Points in Tanzania. A proposed fusion technique was introduced using the maximum likelihood method. The fusion by maximum method means fusion of the DEM which has a better performance for a particular type of terrain and covers. The fused DEM was generated by merging COPERNICUS-1″ and SRTM-1″ through Global Mapper software by considered the DEMs performance in different terrain and land covers. The quality assessment was done using (SD) & (RMS) and were proved that, the fused DEM has better performance than ASTER and SRTM over Tanzania. Also the fused DEM has lower performance compared with COPERNICUS and NASADEM over Tanzania. The RMS results for fused DEM, SRTM, ASTER, COPERNICUS and NASADEM are ±12.173m, ±23.726m, ±18.303, ±3.552 and ±3.648m respectively.

Also in eight selected terrains and land covers the fused DEM has better performance in Flat and bare terrain (Dodoma) and Highlands and forested terrain (Mbeya) over Copernicus, SRTM, ASTER and NASADEM. The RMS results for fused DEM, SRTM, ASTER, COPERNICUS and NASADEM in flat and bare terrain (Dodoma) are ±1.095m, ±20.859m, ±11.123m, ±1.622m and ±2.887m respectively and the RMS results for fused DEM, SRTM, ASTER, COPERNICUS and NASADEM in Highlands and forested terrain (Mbeya) are ±1.496m, ±16.826m, ±14.923m, ±1.848m and ±3.019m respectively.

Keywords: Fused DEM, SRTM, ASTER, COPERNICUS, NASADEM, DEM, GDEM, EGM96, EGM08,WGS84.

TABLE OF CONTENTS

CERTIFICATION ii

DECLARATION AND COPYRIGHT iii

ACKNOWLEDGEMENT iv

DEDICATION v

ABSTRACT vi

TABLE OF CONTENTS vii

LIST OF FIGURES x

LIST OF TABLES xi

ACRONYMS AND ABBREVIATIONS xii

CHAPTER ONE 1

INTRODUCTION 1

1.1 Background 1

1.2 Problem Statement 4

1.3 Research Objectives 5

1.3.1 Main objectives 5

1.3.2 Specific objectives 5

1.4 Scope and Limitations 5

1.5 Significance of the Study 6

1.5.1 Beneficiaries 7

1.6 Outcomes 7

1.7 Hypothesis 7

1.8 Outline 7

CHAPTER TWO 8

LITERATURE REVIEW 8

2.1 Introduction to DEMs 8

2.2 Elevation Data Acquisition 8

2.2.1 Stereoscopy 8

2.2.2 Stereo-photogrammetry 8

2.2.3 Stereo-radargrammetry 10

2.2.4 Interferometry 11
2.2.5 Ranging/Altimetry 12
2.3 DEM Error 14
2.3.1 Error due to land cover and terrain characteristics 14
2.3.2 Error estimation 16
2.4 Global DEMs 17
2.4.1 Multi-source global DEMs 17
2.4.2 Single-source global DEMs 18
2.5 DEM Fusion 19
2.5.1 Fusion with weights 19
2.5.2 Sparse representations 20
2.5.3 Frequency domain filtering 21
2.5.4 Self-consistency 22
2.5.5 Multi-scale stochastic smoothing 23
2.5.6 The maximum likelihood 23
2.6 Vertical Accuracy Assessment 23
CHAPTER THREE 25
METHODOLOGY 25
3.1 The procedures that used in vertical assessment of fused DEM from GDEMs using GPS Ground Controls 25
3.1.1 The distinct areas selected for comparison, performance assessment and validation of GDEMs in Tanzania before fusion 25
3.1.2 Conversion of GGCPs Ellipsoidal Heights to EGM96 Orthometric Heights 30
3.1.3 Fusion of Public GDEMs 30
3.1.4 Extraction of heights from Golden Surfer Software 31
3.1.5 Validation of the fused DEMs using GPS Ground Control Points 31
3.1.6 Comparison of the fused DEM and four GDEMs in Countrywide. 32
3.1.7 Statistical assessment of height differences between fused DEM and GGCPs within the (AOI). 32
3.2 Data requirement, preparation and management 33
3.3 Software used 35
CHAPTER FOUR 36
RESULTS, ANALYSIS AND DISCUSION 36
3.1 RESULTS 36

3.1.1 The statistical difference between fused DEM, four GDEMs using GGCPs in eight representative terrain and land covers 36
3.1.2 The statistics of height difference between fused DEM vs GGCPs and four GDEMs vs GGCPs countrywide 39
3.1.3 The statistics of height difference between fused DEM and four selected public GDEMs Countrywide 40
3.2 DISCUSSION OF RESULTS 41
3.2.1 Performance of Public GDEMs in eight selected types of terrains and land covers 41
3.2.2 General Performance of Fused DEM with GDEMs in Tanzania 42
CHAPTER FIVE 43
CONCLUSION AND RECOMMENDATION 43
3.3 Conclusion 43
3.4 Recommendation 43
REFERENCES 44
APPENDIX 51

LIST OF FIGURES

Figure 1: A map of Tanzania show the distribution of GGCPs 6
Figure 2: 3D view of flat and bare terrain in Dodoma 26
Figure 3: 3D view of a mountainous and forested area in Kilimanjaro and Arusha 26
Figure 4: 3D view of a forested and fairly terrain in Tanga 27
Figure 5: 3D view of a flat and plain terrain in Tabora 27
Figure 6: 3D view of highland and forested area in Mbeya 28
Figure 7: 3D view of Slightly mountainous and forested area in Morogoro 28
Figure 8: 3D view of Flat and forested coastal low land terrain in Lindi 29
Figure 9: 3D view of Barely flat and forested coastal terrain in Mtwara. 29

LIST OF TABLES

Table 3.1: shows the websites used for accessing online data 33
Table 4.1: Shows the Symbols representing the 8 types of terrains and land covers. 36
Table 4.2: Shows the statistics of height difference between fused DEM vs GGCPs and four GDEMs vs GGCPs in A1. 37
Table 4.3: Shows the statistics of height difference between fused DEM vs GGCPs and four GDEMs vs GGCPs in A2. 37
Table 4.4: Shows the statistics of height difference between fused DEM vs GGCPs and four GDEMs vs GGCPs in A3. 37
Table 4.5: Shows the statistics of height difference between fused DEM vs GGCPs and four GDEMs vs GGCPs in A4. 38
Table 4.6: Shows the statistics of height difference between fused DEM vs GGCPs and four GDEMs vs GGCPs in A5. 38
Table 4.7: Shows the statistics of height difference between fused DEM vs GGCPs and four GDEMs vs GGCPs in A6. 38
Table 4.8: Shows the statistics of height difference between fused DEM vs GGCPs and four GDEMs vs GGCPs in A7. 39
Table 4.9: Shows the statistics of height difference between fused DEM vs GGCPs and four GDEMs vs GGCPs in A8. 39
Table 4.10: Shows the statistics of height difference between Fused DEM vs GGCPs and four GDEMs vs GGCPs countrywide. 40
Table 4.11: Shows the statistics of height difference between fused DEM and four public GDEMs Countrywide. 40

ACRONYMS AND ABBREVIATIONS

ALOS	Advance Land Observing Satellite
GDEMs	Global Digital Elevation Models
GPS	Global Positioning System
MERIT	Multi-Error Removed Improved Terrain
DEMs	Digital Elevation Models
AW3D	ALOS World 3D-30m
RADAR	Radio Detection and Ranging
GNSS	Global Navigation Satellite System
SRTM	Shuttle Radar Topography Mission
TanDEM-X	TerraSAR-X add-on for Digital Elevation Measurement
GGCPs	GPS Ground Control Points
VD	Vertical Datum
EGM08	Earth Gravitational Model of 2008.
ASTER	Advanced Space Borne Thermal Emission and Reflection Radiometer.
GGCPs	GPS Ground Control Points.
SAR	Synthetic Aperture Radar.
NASA	National Aeronautics and Space Administration.
WGS84	World Geodetic System of 1984.
AOI	Area of Interest.
NIMA	National Imagery and Mapping Agency.
EGM96	Earth Gravitational Model of 1996.
FDEM	Fused Digital Elevation Model.
RMS	Root Mean square.
SD	Standard Deviation.
USGS	United States Geological Survey.
UTM	Universal Transverse Mercator.

CHAPTER ONE

INTRODUCTION

1.1Background

A Digital elevation model (DEM) is a stereoscopic representation of the Earth's topography, usually in the form of a regular digitized grid (Rishikeshan et al., 2014.). It plays an essential role in hydrology, meteorology, geology, resources censuses and other similar applications (Azzaro, 2012). In order to employ DEMs in geoscience research and applications, it is necessary to generate highly accurate DEM data. In recently years, many public global and quasi-global DEM datasets have become available, such as Shuttle Radar Topography Mission Digital Elevation Model (SRTM DEM), the ALOS Global Digital Surface Model "ALOS World 3D" (AW3D), TerraSAR-X add-on for Digital Elevation Measurement (TanDEM-X) and Multi-Error Removed Improved Terrain (MERIT). Also, DEMs can be acquired from digitized topographic maps, data collected with GPS receiver or total station levelling and digital aerial photographs or satellite images (Elkhrachy, 2018).

Due to advancement of technology different Public Global DEMs covering a large portion of the Earth are being produced with different resolutions. Some of these Public Global DEMs are GTOPO30, COPERNICUS-1″, NASADEM-1″, GLOBE, ETOPO2(2001), ETOPO5, ACE2 (2008), ASTER2 (2011), SRTM3″-CGIAR-CSI v4.1 (2008), SRTM-3″ original (2000), SRTM-1″-v3 (2014), ALOS-1″-v2 (2015), MERIT-3″ (2017), TanDEM-X-3″ (2008) and TanDEM-X-0.4″. In this research four Public Global DEMs are used, these are SRTM-1″-v3, COPERNICUS-1″, NASADEM-1″andASTER-1″, the brief description of four GDEMs are presented in the next paragraphs.

The SRTM-1″-v3 (Shuttle Radar Topography Mission 1 arc-second version 3) is a high-resolution digital elevation model (DEM) dataset that provides detailed topographic information of the Earth's surface. It is an upgrade to the original SRTM dataset, aiming to improve the accuracy and resolution of elevation data. The SRTM-1″-v3 dataset is derived from the Shuttle Radar Topography Mission, which was conducted in February 2000 by NASA's Space Shuttle Endeavour. During this mission, an interferometric synthetic aperture radar (InSAR) system was used to collect radar measurements of the Earth's surface, allowing the creation of a global elevation model. The SRTM-1″-v3 dataset has a horizontal resolution of approximately 1 arc-second, which corresponds to about 30 meters at the equator (Farr, 2007). It provides a detailed representation of the Earth's topography, including mountains, valleys,

and other terrain features. The dataset covers the entire land surface of the Earth between 60 degrees north and 56 degrees south latitude. The accuracy of the SRTM-1″-v3 dataset has been improved compared to the original SRTM dataset through the use of advanced processing techniques and additional data sources (Reuter et al., 2009). It incorporates data from various sources such as the TanDEM-X mission, which is a follow-up radar mission conducted by the German Aerospace Center (DLR).

COPERNICUS DEM, also known as the Copernicus Digital Elevation Model, is a high-resolution elevation model of the Earth's surface developed by the European Space Agency (ESA) as part of the Copernicus program. It provides detailed information about the topography and elevation of various regions. The Copernicus DEM is generated using data from different sources, including satellite and airborne remote sensing, as well as ground-based measurements. These sources include missions such as the Shuttle Radar Topography Mission (SRTM), the Advanced Spaceborne Thermal Emission and Reflection Radiometer (ASTER), and the Global Digital Elevation Model (GDEM). The main purpose of the Copernicus DEM is to support a wide range of applications, including environmental monitoring, urban planning, infrastructure development, and disaster management. It enables users to analyze and model the Earth's surface at a global scale with high accuracy and detail (Azzaro, 2012).

NASADEM (NASA Digital Elevation Model) is a high-resolution global digital elevation model created by NASA using a combination of satellite and airborne radar data. It provides detailed information about the Earth's topography and elevation. The NASADEM dataset is generated using data from the Shuttle Radar Topography Mission (SRTM) and the Advanced Spaceborne Thermal Emission and Reflection Radiometer (ASTER) (Farr, 2007). These missions collect data using radar and optical sensors, respectively, to capture the Earth's surface elevation and characteristics. The SRTM data used in NASADEM is obtained from the onboard radar system of the Space Shuttle Endeavour during a 11-day mission in February 2000 (Farr, 2007). It provides elevation measurements with a spatial resolution of approximately 30 meters globally, covering most land areas of the Earth. The ASTER data used in NASADEM is acquired by the ASTER instrument onboard the Terra satellite. It captures high-resolution optical imagery and stereo-pairs that allow for the derivation of elevation data. ASTER data supplements the SRTM dataset by providing more detailed elevation information for certain areas, especially in rugged terrains and mountainous regions (Farr, 2007). The NASADEM dataset is widely used in various scientific, environmental, and geospatial applications. It

supports research in areas such as hydrology, geology, climate modeling, land cover analysis, and natural resource management (Farr, 2007).

ASTER (Advanced Space borne Thermal Emission and Reflection Radiometer) DEM (Digital Elevation Model) is a digital representation of the Earth's surface topography derived from the ASTER sensor aboard the Terra satellite. It provides detailed elevation data that is widely used in various applications such as topographic mapping, landform analysis, hydrological modeling, and environmental assessment. ASTER DEM is generated by processing the stereo-pair images acquired by the ASTER sensor (Tachikawa et al., 2011). The sensor captures images in three different spectral regions, including visible, near-infrared, and thermal infrared, allowing for accurate elevation measurements. The stereo-pair images are acquired from slightly different angles, enabling the calculation of elevation using stereo photogrammetric techniques. The accuracy of ASTER DEM varies depending on factors such as terrain type, slope, and vegetation cover. Generally, it provides a vertical accuracy of around 20 meters at 95% confidence level for flat to moderately sloping terrain, while the accuracy can be higher for rugged terrain. ASTER DEM data is freely available to the public and can be accessed through various online platforms and data repositories (Abrams et al., 2002). It is widely used in scientific research, resource management, and geospatial analysis. Some common applications of ASTER DEM include flood modeling, geological mapping, glacier monitoring, and urban planning (Farr & Kobrick, 2001).

Previously studies have shown that TanDEM-X-3″ is better than ALOS-1″-v2, MERIT-3″ and SRTM-1″-v3 for some selected types of terrain and land covers such as in flat terrain, forested terrain and the other types of terrain and land cover compare to other GDEM (Mapunda, 2019). So, there is presence of poor performance on other GDEMs caused by terrain characteristics and land cover errors, therefore we need a better DEM which is best fit for all type of terrain and land cover. Therefore, in this study, fusion of SRTM-1″-v3, COPERNICUS-1″, NASADEM-1″and ASTER-1″ based on their performance in eight types of terrains and land covers is conducted.

DEM fusion is an important application case of data fusion in remote sensing (Schmitt and Zhu, 2016; Bagheri et al., 2017). It stems from ongoing developments in remote sensing image fusion, and mostly occurs at the pixel level. According to Papasaika et al. (2008), the fusion of overlapping DEMs acquired via different techniques or at different periods enables the detection of inconsistencies, eliminates gaps in the data coverage and leads to improvement of

the density and accuracy of the datasets. Since DEMs differ in their geometric characteristics, accuracy levels, spatial resolution, temporal resolution, and coverage, data fusion helps to combine the advantages of the different data sources to provide a value-added product that is more complete, accurate and reliable (Karkee et al., 2008). The practice of fusing multi-source and multi-sensor DEMs with variable spatial coverages has been well reported in the literature, and several techniques have been developed and applied by researchers over the years. DEM fusion can be viewed as an ill-posed problem. A problem is said to be ill-posed in the following situations: if the solution to the problem is not unique; if the problem does not have a solution; or, if the result can be significantly altered by a small change in the input data (Hadamard, 1902; Beyerer et al., 2008; Sadeq et al., 2016). There are several situations where the fusion of DEMs is required. For example, for merging of DEMs generated with different technologies, updating DEMs with more recent ones, enhancing DEMs using available auxiliary elevation data from other DEMs, improvement of DEM accuracy through the removal of systematic errors, and fusion of InSAR DEMs with varying acquisition geometries. The integration of mutually independent DEMs can lead to much more semantic information about terrain geomorphology (Podobnikar, 2005). The goal in DEM fusion is to achieve a continuous, contiguous and complete representation of the terrain. For a detailed explanation of situations requiring DEM fusion, see Buckley & Mitchell (2004).

1.2 Problem Statement

Numerous studies have examined the validation, comparison, performance and vertical accuracy assessment of various Global DEMs in Tanzania. These investigations have revealed that certain Public DEMs exhibit poor performance in a specific terrains and land covers types, while others demonstrate superior performance. The poor performance of these DEMs can be attributed to errors arising from terrain characteristics and land covers inaccuracies. Consequently, there is a pressing need for an enhanced DEM solution. This research aims to address the fusion of multiples DEMs to generate a reliable and accurate Fused DEM tailored to the eight selected terrain types in Tanzania. This Fused DEM is expected to be suitable for a wider range of applications, including hydrological modeling, topographic mapping, terrain visualization, land use planning, flood risk assessment and natural resources management.

1.3 Research Objectives

1.3.1 Main objectives

To determine the vertical assessment of fused DEM from ASTER-1″, COPERNICUS-1″, NASADEM-1″ & SRTM-1″-v3 public GDEMs using GPS ground controls in Tanzania.

1.3.2 Specific objectives

The specific objectives are: -

- Statistical analysis of the fused DEM using the GPS ground control points.
- To identify and correct errors or inaccuracies in the fused DEM by comparing it to other existing DEMs and by visual inspection.

1.4 Scope and Limitations

The area of interest covers 1°N to 12°S and 29°E to 41°E with eight various types of terrains and land covers namely flat and bare terrain, mountainous and forested terrain, flat and forested coastal low land terrain, high lands and forested terrain, slightly mountainous and forested terrain, bare flat and forested coastal terrain, forested and fairly flat terrains. The GPS Ground Control Points are not everywhere i.e., not at every grid intersection, therefore the Fused DEM is assessed where the controls are. The research limited to the vertical accuracy, it may not cover other aspects such as horizontal accuracy and temporal resolution. Figure 1 below shows the study area and the distribution of the GPS Ground Control Points on the World Geodetic System of 1984 (WGS84).

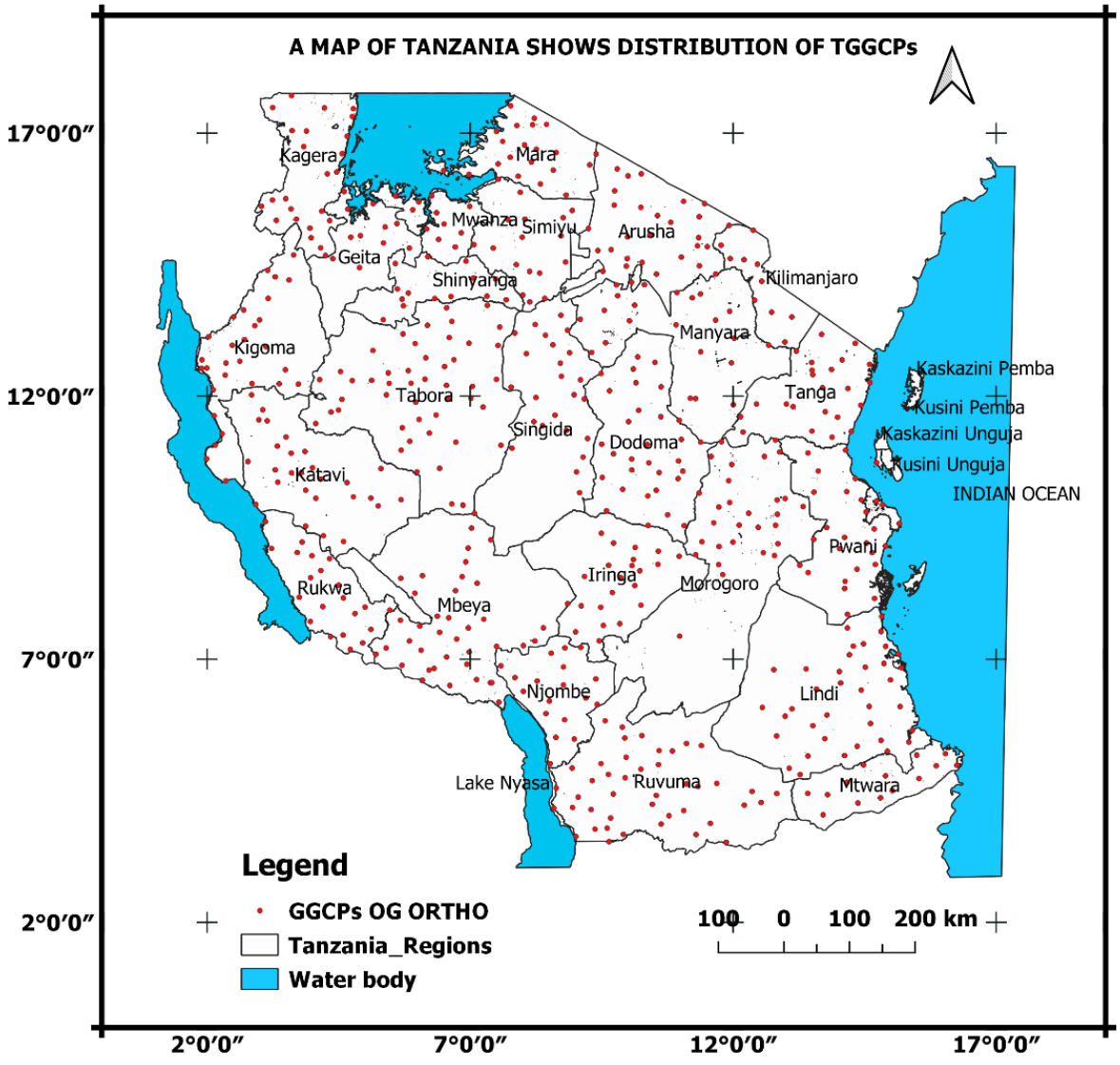

Figure 1: A map of Tanzania show the distribution of GGCPs

1.5 Significance of the Study

a) This research will help to derive fused DEM for Tanzania mainland from Global Digital Elevation Models.

b) This research will help to ensures that the data is reliable and accurate, which is crucial for various applications.

c) This research will help to determine the level of agreement or discrepancy between fused DEM and GGCPs or between fused DEM and other GDEMs.

1.5.1 Beneficiaries

This study extends its benefits to various professionals, including geodesists, geomaticians, engineers, agriculturalists, military personnel, mariners, and environmental divisions, such as those involved in vegetation monitoring. It encourages them to avoid relying solely on field data by demonstrating the potential of utilizing DEM (Digital Elevation Model) data in areas where traditional sources of elevation data may not be accessible. As a result, these beneficiaries can now supplement their analyses and decision-making processes with valuable DEM data to enhance their work.

1.6 Outcomes

The main outcome of this research is fused DEM, also the statistics of height differences between fused DEM vs Public Global DEMs and fused DEM vs GPS Ground Control Points.

1.7 Hypothesis

It is hypothesized that; Fused DEM will provide better results compared to selected four GDEMs in the selected terrain and land covers when they are determining the assessment of vertical accuracy using GPS Ground Control Points on AOI.

1.8 Outline

This dissertation contains five chapters. Chapter one is an introduction to the study, providing an overview of the research context, research problem, objectives, significance, beneficiaries, scope and limitations and outcomes. Chapter two contains a literature review on elevation data acquisition, error assessment, globally available DEMs, and DEM fusion strategies and results. Chapter three contains a description of the methods used to determine the vertical assessment of fused DEM from ASTER-1″, COPERNICUS-1″, NASADEM-1″ & SRTM-1″-v3 public GDEMs using GPS ground controls in Tanzania. Chapter four provides the results of the fused DEM as well as and the results of the input DEM and also contains a discussion of the results presented. The conclusions and recommendation of the thesis study are in Chapter five. Additional tables for the thesis are provided in Appendix.

CHAPTER TWO

LITERATURE REVIEW

2.1 Introduction to DEMs

A digital elevation model (DEM) is a regularly spaced grid which contains the elevation of a point on a surface that is coincident with the location of the grid cell. Often DEMs are also referred to as a DTM (digital terrain model), or a DSM (digital surface model) (Poon et al. 2005). The data used to create an elevation surface can be acquired using various technologies and at different scales. Traditionally elevation data was acquired through ground-based surveying methods. The development of remote sensing technologies has enabled elevation data to be derived more quickly and at a greater scale than before. Remote sensing techniques have also provided elevation data for areas that are difficult to access and survey (Gao, 2007).

2.2 Elevation Data Acquisition

Elevation data acquisition refers to the process of capturing, measuring, and collecting information about the vertical height or elevation of the Earth's surface. The main methods used to derive elevation estimates from remote sensing data are stereoscopy, interferometry, and ranging (also known as altimetry) (Hopkinson et al., 2009; Weschler, 2007). This data is crucial for various applications, such as cartography, geographic information systems (GIS), urban planning, environmental modeling, and disaster management. Understanding the elevation of terrains, mountains, valleys, and water bodies is essential for creating accurate maps, conducting analyses, and making informed decisions in a wide range of industries (Toutin & Gray, 2000).

2.2.1 Stereoscopy

By viewing two images that are acquired from different angles the disparity in the location of features can be seen as displacement and therefore a third dimension (i.e. elevation) can be observed. This method of extracting elevation is stereoscopy, and is built on principles that relate to the depth perception capabilities of a pair of human eyes (Toutin & Gray, 2000).

2.2.2 Stereo-photogrammetry

The use of images from film, digital cameras, or digital scanners to characterize features is called photogrammetry. Techniques of photogrammetry include clinomtery and stereoscopy;

the latter being more commonly used for elevation extraction (Toutin & Gray, 2000). Initially stereoscopy involved viewing stereo pairs of aerial photographs through a stereoviewer. For this technique the accuracy of elevations derived depends on the altitude at which the photographs are taken and the characteristics of the features observed (Lillesand et al., 2008).

Originally aerial photographs were taken with film, but the development of digital cameras allowed the process to be taken into a computer environment. Computer-based stereo workstations were developed, with which users could view the images and see the features in 3- D. Eventually, this included satellite imagery when digital scanners were employed on satellites (Toutin & Gray, 2000).

The most common stereo-photogrammetry procedure currently used involves image matching computer programs which have replaced the stereo workstations. Images are matched and adjusted either in pairs or blocks of several images with the use of tie points – this is referred to as bundle or block adjustment. By knowing the internal geometry of the camera (i.e. focal length, lens distortion) and the external geometry of the image acquisition (altitude of the platform, angle of nadir relative to the ground surface) the image parallax can be calculated for each matched pixel (Lillesand et al., 2008). Topography can be determined from the parallax in the two images since targets at different heights are displaced by an amount related to their elevation (Leberl, 1990, in Rosen, et al., 2000).

Residual error within the elevation model can be estimated with independent check points (ICPs). If the estimated error is too high then the GCPs can be modified (Gao, 2007). Computation of the elevation model from the image parallax allows relative elevations to be calculated. To achieve absolute elevations a number of ground control points (GCPs) with known horizontal and vertical coordinates are required (Gao, 2007).

Aerial photography can be used to produce DEMs with a vertical accuracy of less than a metre, whereas those derived from satellite imagery are in the range of 3 to10 m in the case of IKONOS (Poon et al., 2005) and Quick Bird (Toutin, 2004). DEMs generated from automatic stereo image matching (e.g. optical or RADAR) often, however, contain large erroneous blunders due to incorrectly identified match pixel pairs (Milledge et al., 2009a). As well, DEMs derived from optical stereo images specifically can be inhomogeneous since they depend on image feature contrast, and are also compromised by cloud cover (a major issue in the tropics) and lack of sunlight in some cases (Rabus et al., 2003).

2.2.3 Stereo-radargrammetry

Radargrammetry involves images acquired from active, RADAR (Radio Detection and Ranging) sensors, instead of cameras in the case of photogrammetry. There are several advantages of working with RADAR systems rather than optical, passive systems, such as digital cameras. Radar operates with the use of microwave energy allowing electrical and geometrical properties of surfaces to be represented. Operating at this wavelength also allows for all weather operation due to the ability of microwaves to penetrate clouds (Bamler & Hartl, 1998; Toutin & Gray, 2000). Because the RADAR system provides its own source of illumination (an active system) it can operate both day and night. (Rosen et al., 2000; Toutin & Gray, 2000).

Stereo-radargrammetry is similar to stereo-photogrammetry, except that Synthetic Aperture RADAR (SAR) sensors are used instead of cameras. With traditional RADAR the antenna length is a limiting factor in the azimuthal resolution that can be achieved with increasing range. SAR is a technology which solves the issue of a limited antenna length by transmitting pulses ahead of the sensor and receiving the pulses further along in the course of the aircraft or satellite (Bamler & Hartl, 1998). A SAR image pixel can contain the amplitude (energy intensity) as well as the phase (time delay) of the signal (Smith, 2002). Only the amplitude portion of the signal is utilized in stereo-radargrammetry; the phase is utilized in InSAR methods (Bamler & Hartl, 1998; Smith, 2002). SAR data is useful not only for deriving elevations, but also for other areas of research including that of polar ice, vegetation, biomass estimation, and soil moisture mapping (Rosen et al., 2000). SAR technology is implemented on both aerial and satellite platforms.

Advances in stereo-radargrammetry have recently been achieved with higher resolution modes on satellites such as RASARSAT-2 (Ultra-fine mode is 3x3 m pixel imagery), as well as 10 improved 3-D radargrammetric models. These models incorporate precise satellite orbiting geometry, and reduce the need for GCPs (Toutin & Chénier, 2009). Toutin & Chénier (2009) tested a new version of Toutin's 3-D radargrammetric model on RADARSAT-2 Ultrafine Mode imagery and were able to produce a DEM with an accuracy of 1 m horizontally and 2m vertically when compared to DEMs created from orthophotos. Though aerial SAR imagery is capable of producing higher resolution DEMs, the limitation of this method is the extent that can be acquired and the cost of the survey. The recent advances in satellite SAR stereo-

radargrammetry can allow for a much greater extent of DEM creation than aerial surveys, with accuracies that are not much lower.

Similar to stereo-photogrammetry, the main cause of large blunders (i.e. spikes or pits) in elevation estimates in stereo-radargrammetric DEMs is pixel matching error (Fayard et al., 2007). Poor correlation between image-pair pixels can result from changes in the backscatter amplitude due to target change between image acquisitions (Toutin, 1998), from speckle that is inherent in most RADAR images (Ostrowski & Cheng, 2000), or is due to a lack of texture in the imagery (Paillou & Gelautz, 1999).

2.2.4 Interferometry

Interferometric SAR is usually called InSAR, and sometimes referred to as IFSAR or ISAR (Rosen et al., 2000). InSAR technology uses SAR phase information, rather amplitude data which is used in stereo-radargrammetry (Rosen et al., 2000; Smith, 2002; Toutin & Gray, 2000). The InSAR viewing geometry for a certain point on the ground involves two SAR antenna positions separated by a baseline (i.e. short distance) and the ground location. Each SAR 11 antenna measures the phase, which is related to the number of wavelengths of the signal needed to cover the distance from the antenna to the ground and back to the sensor (Smith, 2002).

There are three possible configurations for the two InSAR antennas: across-track, along-track, and repeat-pass. In each technique the phase of one antenna is subtracted from the other for each pixel in the image pair resulting in an interferogram. The difference in phase is related to the baseline and surface relief (Smith, 2002).

Across-track interferometry involves using two antennas on the same platform (Madsen et al., 1993), while along-track interferometry uses two satellites following each other closely. The phase difference in both techniques is related to the parallax caused by different acquisition angles (Smith, 2002). The sensitivity to terrain topography increases with the baseline distance, reaching an optimal baseline for generating digital elevation models (DEM) (Toutin & Gray, 2000).

Repeat-pass technique requires the sensor to pass over the same area with nearly identical viewing geometry for two passes (Smith, 2002; Toutin & Gray, 2000). When this condition is met, the phase difference relates to a change in elevation at a specific point. Interferometry is highly accurate for acquiring elevation data, with accuracy measured in wavelengths (Smith, 2002).

Challenges in InSAR technology include phase unwrapping and pixel decorrelation. Phase unwrapping involves adding the appropriate number of phases to determine the true slant range of the radar signal interacting with the target (Rabus et al., 2003). Various methods exist for phase unwrapping (Bamler & Hartl, 1998). Decorrelation refers to the reduction of coherence between two SAR images, commonly occurring when target orientation changes between acquisitions (Zebker & Villasenor, 1992; Reinartz et al., 2005).

InSAR technology offers higher accuracy in elevation values compared to stereo-radargrammetry, with millimeter to centimeter accuracy possible depending on the platform and sensor (Rosen et al., 2000). InSAR also benefits from automated processing, requiring less user interaction compared to stereoscopy (Madsen et al., 1993; Rosen et al., 2000; Toutin & Gray, 2000). Airborne InSAR can achieve horizontal accuracy below a meter, suitable for hydrological applications (Bamler & Hartl, 1998). Satellite InSAR sensors typically have a horizontal accuracy of around 25 meters, making them more suitable for applications like sea ice monitoring and tectonic activity (Gao, 2007).

A ground-based InSAR unit has been developed with a longer synthetic aperture achieved by sliding the transmitting and receiving antennas along a track (Nico et al., 2004). This technology was used to create a DEM for a 3 km by 1 km test site, with an RMS of 5 meters compared to an existing DEM (Nico et al., 2005). It is potentially useful for localized, large-scale terrain modeling.

2.2.5 Ranging/Altimetry

One way of acquiring a high-quality DEM is by employing Light Detection and Ranging (LiDAR) technology. LiDAR is a type of ranging technology that is sometimes referred to as laser altimetry. Similar to other active sensors such as RADAR, LiDAR involves the transmission of pulse of energy from a source, the pulse reflecting off a feature, travelling back toward the platform and being received by a sensor (Wehr & Lohr, 1999). The laser wavelength is in the near-infrared range of the electromagnetic spectrum giving LiDAR an advantage that the signal is quite reflective off of natural surfaces and it is more eye-safe than other visible wavelengths (Hopkinson, 2006). The way that the backscatter is recorded is either as a waveform (when the signal is sent as a continuous wave) or as discrete returns (when the signal is sent as a series of pulses) (Bortolota & Wynne, 2005; Hopkinson, 2006). First and last returns of discrete returns can be separated, or the full waveform of a continuous wave can be analysed,

to help differentiate the ground location from that of off-terrain objects (Coveney & Fotheringham, 2011).

Often the LiDAR system is mounted on an airborne platform, though ground-based units and satellite sensors are also utilized. A relative coordinate and range of each point is determined using the speed of light, the location and orientation of the source at the time of transmission, and the time between laser pulse transmission and reception (Wehr & Lohr, 1999). In the case of airborne LiDAR, relating the relative coordinates and ranges of the pulse returns to the aircraft trajectory enables the survey points to be translated to ground coordinates with elevations (Hopkinson & Demuth, 2006). This is achieved with an Inertial Motion Unit (IMU), coupled to a high-precision GPS unit, which has enabled the high-precision of LiDAR data acquisition 14 (Hopkinson, 2006). The exact precision depends on the survey conditions, but is generally in the range of tens of centimetres (Gao, 2007).

Another advantage of airborne LiDAR is its ability to penetrate forest canopy and other heavily vegetated areas since the pulse (especially small-footprint LiDAR) can pass through relatively small gaps in the ground cover (Wulder et al., 2008). Since aerial LiDAR datasets can produce fine-resolution, high accuracy DEMs they are also useful for assessing the accuracy of other methods of elevation extraction (Toutin et al. 2010). The main disadvantage to aerial LiDAR though, is that it is a relatively expensive method of acquiring elevation data and surveys are often limited to small study areas (Gao, 2007).

LiDAR technology is also available aboard some satellites, including GEOSAT, SEASAT, and ENVISAT, enabling elevation data to be collected at the global scale (Gao, 2007). One such example, the Shuttle Laser Altimeter (SLA) has a sampling interval of 0.75 m vertically and 0.7 km horizontally, with vertical accuracies of 1 m in gentle terrain, and 11 – 46 m in rugged terrain (Garvin et al., 1998). Another example is the Geoscience Laser Altimeter System (GLAS) sensor aboard the Ice, Cloud and land Elevation Satellite (ICESat) that collects LiDAR data with 70 m footprints, spaced 170 m apart. The accuracy of GLAS data is reported to be better than 0.3m (Reuter et al., 2009).

Ground-based LiDAR units are sometimes referred to as Terrestrial Laser Scanners (TLS). They also utilize high accuracy GPS to relate the scan points to a real-world reference system, but do not incorporate an IMU unless they are employed on a moving vehicle (usually TLS systems are stationary). The angle of acquisition is more oblique to the ground surface compared to that of airborne or satellite-based systems, and for this reason multiple scans of

terrain from 15 different directions or azimuth angles are required to minimize the effect of occlusion. Ground-level vegetation can be a particularly challenging source of occlusion for TLS systems (Coveney & Fotheringham, 2011). TLS systems are more limited in the size of area that can be surveyed compared to the aerial and satellite-based systems, and so they are more suitable to support field-scale elevation data requirements.

2.3 DEM Error

All DEMs contain error that is a result of limited measurement precision, the presence of off-terrain objects in the acquisition area, and interpolation (Lindsay, 2006), as well as error that occurs during data processing (Wechsler, 2007). Also, errors in acquisition can be caused by the characteristics of the terrain or land cover, for example: the moisture content of soil or vegetation, the slope or aspect of topography, and the roughness of surfaces (Bater & Coops, 2009; Reuter et al., 2007; Toutin, 2002). Error can also be propagated if an unsuitable interpolation method is chosen to process the DEM.

2.3.1 Error due to land cover and terrain characteristics

Some forms of error in data acquisition and elevation extraction are unique to the sensor being employed, such as that caused by limited measurement precision, or during the processing of data. There are other errors in data acquisition which are more common amongst sensors though: signal scattering, occlusion, attenuation and multipath. These errors can be propagated into the DEM created from the acquired data (e.g. imagery).

Slope and the orientation of slope (i.e. aspect) can affect how much of the instrument signal is reflected back to the sensor. Toutin (2002) conducted a study on how accuracy relates to the 16 slope and aspect of terrain in a DEM derived from RADARSAT image stereo-pairs. He found that stereo-radargrammetric DEM error was linearly related to slope, with steeper terrain causing more error. This error is due to radiometric disparity in the images (differences in signal amplitudes for the same pixel location in two images) causing image matching errors. Li et al. (2006) conducted a study using ERS data and also found that DEM error increased linearly with the slope of the terrain. As well, Toutin (2002) also found that topographic aspect (orientation of slope with respect to the position of the sensor) played a minor role in error, with fore-slopes being more accurate, and back-slopes being less accurate.

Specular reflection can cause the transmitted signal to be entirely reflected away from the instrument resulting in none of the energy returning to the sensor. A good example of a surface

that causes this is still water, since it can cover a large portion of the terrain at times and can be very smooth. Specular reflection can occur in passive optical systems when the sun is at a low angle to the terrain compared to the sensor (Lillesand et al., 2008), or in active systems such as LiDAR (Hopkinson, 2006) and SAR (Reuter et al., 2007), when the transmitted signal is reflected completely away from the sensor. Denker (2005) reported that water bodies were not well defined in the initial version of SRTM3 data since they cause a low amount of RADAR backscatter. Reflection away from the sensor results is a loss of data for the surface that was the cause of the reflection. In the case of surface water, this is not necessarily a major issue for DEM creation since the elevation of the water surface is usually the same throughout.

Occlusion is another cause of missing elevation data, except in this case the data can be missing for non-uniform areas of elevation. Occlusion is caused when the signal is reflected off of a feature before it is able to reach an area of interest. In a sense, an object blocks the line-of sight for the instrument. It can occur in terrain of steep relief, in heavily vegetated areas, or urban 17 centres amongst other cases (Lillesand et al., 2008). The area in the 'shadow' of the occluding object is simply missing from the acquired data. As an example, Coveney & Fotheringham (2011) discuss the issues of occlusion due to dense ground vegetation when using a TLS system. Also, Denker (2005) notes the absence of SRTM3 data in the Alps where the mountains are high and there are narrow gorges.

Attenuation occurs when the medium that the signal is travelling through absorbs the energy of the signal. Moisture in soil or vegetation is a common cause of signal attenuation (depending on the signal wavelength). Attenuation can occur in LiDAR (Hopkinson, 2006), RADAR (Dobson & Ulaby, 1986; Reuter et al., 2007), and optical systems (Lillesand et al., 2008). It should be noted that high soil moisture, measured as bulk water differentiated from bound water, can increase the backscatter for RADAR, rather than attenuate the signal (Dobson & Ulaby, 1986). For elevation derived from image pairs, attenuation can cause image matching errors if there is a change in conditions between images. In the case of LiDAR, severe attenuation will cause data drop-outs (Hopkinson, 2006).

Multipath errors cause a much different effect than the aforementioned errors in data acquisition. Multipath occurs when the signal of an active instrument is reflected off of more than one surface before returning to the sensor (Hopkinson, 2006). The assumption of the instrument is that the signal will travel in a straight line to and from a target. When this does not happen, the increased time in transmission and reception of the signal translates into an

increased range. The information recorded for that location then has either an erroneous elevation or intensity (Lillesand et al., 2008). Situations that cause multipath include corner reflection from angular, highly reflective features such as buildings (Stilla et al., 2003), and where trees or other heavy vegetation over-hang surface water (Townsend, 2002).

2.3.2 Error estimation

DEM error is usually estimated using a more accurate reference dataset such as GPS points (Coveney & Fotheringham, 2011; Gao, 2007) or other DEMs (Fisher and Tate, 2006). The most widely used measure of DEM error is the Root Mean Squared Error (RMS) (Aguilar et al., 2005; Desmet, 1997). RMS is the square root of the average of squared differences taken between the DEM being assessed and reference points that are believed to be of higher accuracy (Wechsler, 2007). The equation for RMS is given below:

$$RMS = \sqrt{\frac{\sum_{i=1}^{n}\left(Z_i^{est} - Z_i^{ref}\right)^2}{n}} \quad \text{..... 2.1}$$

Where Z_i^{est} is the estimated elevation and Z_i^{ref} is the reference elevation at location i, and n is the number of residuals calculated (modified from Aguilar et al., 2005). A number of studies have shown that the mean error is not equal to zero, and so the RMS alone is not a good way to describe the statistical distribution of the error (Fisher & Tate, 2006). Fisher & Tate (2006), and Desmet (1997) suggest that at least the Mean Error (ME) and the standard deviation of the error (S) should be reported along with the RMS.

Even though the RMS is the most commonly used estimate of DEM accuracy Weschler (2007) as well as Fisher & Tate (2006) stated that it is not necessarily the most appropriate. The RMS assumes that DEM errors are random, and that they are normally distributed in their values, which is not true of most DEMs. The RMS also does not reflect how well each cell of the DEM reflects the true elevation (Wechsler, 2007). Weschler further argues that error would be better represented in a probability map, and that the contribution of error sources should be quantified to allow for a better understanding of the nature of the error.

Fisher & Tate (2006) argue that the RMS, ME, and S all fail to represent the spatial pattern of error, which is an important consideration in DEMs since error tends to be spatially correlated. As a solution they recommend that either unconditioned or conditioned error models be used. Unconditioned error simulation models use stochastic simulations of random function

realizations that can be applied to the DEM, often through the use of a Monte Carlo simulation method. They are based on properties of the error distribution but actual estimates of error are not honoured. The assumption of unconditioned error simulation models is that the error pattern is uniform over the entire DEM, which is often not the case. Conditional error simulation models differ in that they honour the estimates of error at particular locations and therefore do not assume that the error pattern is uniform (Fisher & Tate, 2006).

It is important to note that estimates of error that are based on reference data sets are not actually estimating absolute error from the true ground surface, but rather are discrepancies from the reference data values, since even the most accurate ground truth data contains a certain level 23 of error as well (Gao, 2007). Papasaika et al. (2009) suggest that in the absence of a higher quality reference data set, alternative techniques such as the evaluation of slope, aspect, and roughness, can be used to assess the accuracy of a DEM. Reuter et al. (2009) suggest that even with a reference dataset terrain parameter such as slope and curvature should be evaluated to assess the accuracy of a DEM.

2.4 Global DEMs

The first attempts to create a DEM of the globe involved merging elevation from multiple sources into a single product with the greatest coverage possible. More recent advances in Space borne remote sensing instruments have allowed for near global coverage from single sensors. Examples of both types of global DEMs are briefly reviewed in this section.

2.4.1 Multi-source global DEMs

Initial efforts to create a DEM with global coverage involved the merging of elevation data from multiple sources. Two of the main products that resulted from these efforts were GTOPO30 and GLOBE.

GTOPO30 is a global DEM with a grid spacing of 30 arc seconds (approximately 1 km). It was compiled from eight different elevation data sources and was developed for regional and continental scale topographic data use (Harding et al., 1999). The main data sets and the percentage contributing to GTOPO30 for land areas were: Digital Terrain Elevation Data (DTED, 50%), a 1-degree elevation model for the USA (6.7%), and Digital Chart of the World vector data (DCW, 29.9%) (Miliaresis & Argialas, 2002). The DCW vector data used were24 contours, spot heights, stream lines, lake shorelines and ocean coastlines; all of which were converted to a raster with drainage enforcement (Harding et al., 1999).

Because several raster and vector sources of topographic information were used the accuracy of GTOPO30 varies by location according to the source data (Denker, 2005). For example, Harding et al. (1999) note that the New Zealand DEM RMS is 9 m whilst the Peru map RMS is 304 m. Miliaresis & Argialas (2002) also compare the plus or minus 30 m accuracy of DTED to the plus or minus 160 m accuracy of DCW data in the GTOPO30 DEM. Despite the large variation in elevation accuracy, GTOPO30 data was a major contributor to GLOBE (Hastings & Dunbar, 1998) which was the next global DEM initiative.

The Global Land One-kilometer Base Elevation (GLOBE) DEM was initially an empty 2-dimensional, 30 arc-second array that was opened and the best available data used to fill it. It was developed before the scheduled launch of SRTM (Shuttle RADAR Topography Mission; described in the next section of this literature review) in 1999. The U.S. Defense Mapping Agency contributed DTED Level 0 data, and national elevation datasets were also contributed from Australia, Japan, and New Zealand. As well, GLOBE contained data from the GTOPO30 DEM (Hastings & Dunbar, 1998).

Similar to GTOPO30, GLOBE can be locally quite unreliable since the merged datasets were acquired with a variety of sensors and many different techniques were employed during the elevation generation process (Rabus et al., 2003). Hastings & Dunbar (1998) state that perhaps half of GLOBE exceeds 20m RMS and that the area of Antarctica could be off as much as 300m vertically. They also note that some errors may be from differences in projection and datum since many datasets do not come with proper documentation.

2.4.2 Single-source global DEMs

Advancements in space-borne remote sensing instruments have led to increased global coverage of digital elevation models (DEMs) from single sensors. Examples of such DEMs include SRTM, GDEM, and the upcoming World DEM.

The Shuttle RADAR Topography Mission (SRTM) was conducted in February 2000 and used RADAR data to create a high-resolution topographic database of the Earth between 60° North and 57° South latitude (Rabus et al., 2003). SRTM was the first single-pass interferometer in space, reducing decorrelation by acquiring image pairs under similar atmospheric and ground conditions. The vertical accuracy of the SRTM DEM was reported to be 16 m, but the initial release (SRTM3) had some errors, including voids, spurious points, and poorly defined water bodies (Rabus et al., 2003).

The Global DEM (GDEM) was produced using optical imagery from the ASTER system on the Terrasat satellite (Denker, 2005). Data was collected between 2000 and 2007, resulting in coverage from 83° South to 83° North latitude. GDEM, released in 2009, had a resolution of 30 m and a vertical accuracy of 20 m (Reuter et al., 2009). It provided finer resolution and greater coverage compared to SRTM, but it also had errors, such as systematic strip effects in Australia and unremoved cloud elevations (Hirt et al., 2010).

The anticipated next global DEM is the World DEM, generated from the Tandem-X InSAR system using X-band RADAR. It is expected to have a resolution of 12 m and global coverage from pole to pole. The reported vertical accuracy is 2 m (relative) and 10 m (absolute), as mentioned on the provider's website (Astrium, 2013).

2.5 DEM Fusion

There are several DEM fusion techniques that have been proposed and tested in the literature over the past three decades. Many of these involve simple techniques such as data gap filling, and the weighted averaging of input elevations based on: global measures of error; height error maps from the DEM generation process; terrain derivatives; or combinations thereof. More sophisticated techniques of DEM fusion involve the use of sparse representations, frequency domain filtering, self-consistency in the generation process, or multi-scale stochastic smoothing (Papasaika et al., 2011).

2.5.1 Fusion with weights

The simplest form of DEM fusion is taking the average of all available overlapping DEMs at each cell location. This type of fusion is not satisfactory though, since large errors can skew the average; the magnitude of the error will be reduced but the resultant DEM will still have blunders (Schultz et al., 2002). A more intelligent approach is to apply weights to the elevation estimates based on error probability to control their influence on the fused elevation estimates. Roth et al. (2002) used weighted averaging to fuse the overlapping portions of DEMs derived from MOMS-2P, SRTM-X, and ERS-Tandem imagery. The weights were derived from the image geometry (an estimated overall accuracy), and height error maps from the DEM generation process (an estimated accuracy at each cell location). Also, a statistical outlier test was performed to identify and correct errors in the fused DEM. The results of the fusion were provided as DEMs and maps of estimated height error for a subset of the study area. Roth et al. (2002) reported that the overall quality of the fused DEM was better than the input DEMs.

In a study conducted by Reinartz et al. (2005), different types of digital elevation models (DEMs) were combined to improve their accuracy. The study used SRTM-C and SRTM-X (both InSAR) as well as optical along-track stereo SPOT-5 DEMs. During the generation of InSAR DEMs, height error maps were created based on coherence and density of residuals. These error maps were then used as weights to adjust the SRTM DEM elevations. Similarly, weights for the SPOT-5 DEM estimates were derived from the mean standard deviation and density of matched points in the stereo photogrammetric DEM generation process. The input DEMs and the fused DEMs (both representing DSMs) were compared to a higher accuracy DTM. The study provided statistics such as mean, standard deviation, minimum, and maximum offsets for different land use areas like fields, suburbs, and forests. The fusion DEMs generally had lower standard deviations compared to the input DEMs, except for the fusion of SRTM and SRTM-C DEMs. Maps of the probability of height error also showed significant improvement when all input DEMs were fused.

Another study by Papasaika et al. (2009) presented a more sophisticated technique for fusing DEMs. In this study, weights for fusion were calculated using a combination of a priori information about DEM errors, terrain derivatives of the input DEMs (such as slope, aspect, and roughness), and land use classes derived from IKONOS imagery. The fusion process involved combining DEMs generated from LiDAR data and stereo IKONOS imagery using an active surface model. The model attracted the less accurate surface towards the more accurate one, and the resultant DEM's shape was influenced by the nominal accuracy, generation technique of the input DEMs, and land cover. Internal forces such as accuracy and generation technique, as well as external forces such as geomorphological features, drove the fusion process. The study presented preliminary visual assessments for two subset areas, indicating an improvement in representing hedges and buildings in the fused DEM.

2.5.2 Sparse representations

Building on previous research by the authors, Papasaika et al. (2011) proposed and tested the use of sparse representation theory in DEM fusion. The use of sparse representations would allow DEM fusion to be represented as a mathematical optimization problem that could be solved to global optimality. In this technique the area of interest is segmented into overlying patches of grid cells. Dictionaries of patches (i.e. unique combinations of terrain shape) are 29 created from higher accuracy DEMs in training areas. Error weights calculated from the slope and roughness of the input DEMs are also used in the fusion. The model is optimized to globally

minimize the difference in expected elevations and the input DEMs. This approach was tested on pairs of DEMs, though the authors claimed that it could be extended to more than two DEMs. The three input DEMs were generated from ALOS/PALSAR-2, ERS C-band, and SPOT imagery. A LiDAR DEM was used to corroborate the input and fusion DEMs, and mean offsets as well as RMS values were provided as results. The ALOS-SPOT DEM fusion had a lower mean and RMS compared to the input DEMs, whereas the other fusion pairings had either a lower mean, or a lower RMS than the input DEMs.

2.5.3 Frequency domain filtering

Frequency domain filtering as a method of DEM fusion was first introduced by Honikel in 1998, and has since been tested and published by a few others (Crosetto & Aragues, 2000; Karkee et al., 2008). The basis of this technique is that the lower frequency portion of one DEM (i.e. coarser terrain features) can be isolated and merged with the higher frequency portion of another DEM (i.e. finer terrain features) of the same area. This has been applied to DEMs generated with InSAR and stereo-photogrammetry techniques since the InSAR DEMs tend to be more accurate in the high frequency, and the stereo-photogrammetric DEMs tend to be more accurate in the low frequencies. Frequency domain filtering involves four main steps: converting the DEMs into the frequency domain; applying a low or high pass filter to the appropriate DEM; adding the two desired DEM portions; converting the resultant data back to the spatial domain. Honikel (1998) tested this method on and InSAR DEM generated from ERS imagery, and on a stereo-photogrammetric DEM generated from SPOT imagery. Different cut-off frequencies were 30 applied and, in all cases, the mean offset was the same as the higher accuracy SPOT DEM, but the RMS was lower than that of both input DEMs.

In another study by Crosetto & Aragues (2000) a stereo-radargrammetric DEM generated from RADARSAT-1 imagery and an InSAR DEM generated from ERS-1 imagery were fused using frequency domain filtering. Unfortunately, the DEM fusion was not the focus of the article and so the results of the fusion were not well reported however, the authors did state that the fusion removed systematic errors that were present in the InSAR DEM, and that the DEM precision was also improved.

A more recent study, by Karkee et al. (2008), included a DEM gap filling step before the frequency domain filtering step in the fusion of a stereo-photogrammetric DEM generated from ASTER imagery and an SRTM-C (InSAR) data. The gap filling was necessary since the SRTM DEM contained many holes due to shadow in the RADAR imagery and areas of poor coherence

between images. An erosion technique using the slope and aspect of the SRTM cells surrounding the gap was used to fill the gaps. After the gap filling and frequency domain filtering, the input DEM and fusion DEM were corroborated with a 1:25000 scale contour map of the study area. Karkee et al. (2008) reported that the fused DEM had an RMS that was 42% lower than that of the ASTER DEM, and 10% lower than that of the SRTM DEM. The mean offsets for all DEMs were the same value, due to the co-registration of the input DEMs before fusion.

2.5.4 Self-consistency

Another method of DEM fusion, specific to DEMs generated from stereo-photogrammetry techniques, employs the theory of self-consistency (Schultz et al. 1999, 2002). In this method two DEMs are generated from the same pair of images by switching the reference and target 31 roles for elevation extraction. If the elevation estimates at the same cell location differ by greater than a threshold distance the estimates are not accepted. The threshold is determined by fitting all disparities between the elevations of the DEM pairs to a Gaussian distribution, and threshold is a user specified number of standard deviations from the mean of the distribution.

Schultz et al. (1999) generated 12 DEMs from six pairs of aerial photography images of a barren desert area and applied the self-consistency constraint to filter for reliable estimates. The reliable estimates at each cell location in the study area were simply averaged to create the final fused DEM. The average of each DEM pair (created from the reversal of roles of the imagery) was also created for comparison with the fused DEM. Schultz et al. (1999) reported that the fused DEM was slightly less accurate (measured by the standard deviation of offsets with the ground truth) than the average DEMs generated from three out of five DEM pairs. It was not explained why the results of the sixth DEM pair were not provided. The study by Schultz et al. in 2002 only provided results for five of the original DEM pairs, and not for the fusion product. The fusion strategy was however, applied to DEMs derived from IKONOS imagery over an air force base as an example an urban area, which provided new results. Only visual assessments of the air force base area however were provided for one of the DEM pairs and the fused DEM.

The article by Stolle et al. (2005) was authored by many of the same people that authored the Schultz et al. 2002 paper. In that more recent study (Stolle et al. 2005), the same methodology for self-consistency fusion was applied to a different area of desert, and to 18 DEMs of a different urban setting that contained high-rise buildings. Only visual assessments and graphed

distributions of elevations were provided as results for one of the inputs DEMs and the fused DEM.

2.5.5 Multi-scale stochastic smoothing

A multi-scale Kalman smoothing filter was used by Slatton et al. (2002) to fuse InSAR DEMs of different resolutions. The multi-scale Kalman filter was employed because it considers the stochastic variability in parameters and is optimal with respect to the minimal mean squared error involved in the DEM fusion model. In the Slatton et al. (2002) study, one low resolution InSAR DEM derived from ERS1/2 imagery was fused with three higher resolution InSAR DEMs generated from TOPSAR imagery. The resultant fused DEM of the ERS DEM fusion with the first TOPSAR DEM was then fused with a second TOPSAR DEM, and that resultant DEM was fused with a third TOPSAR DEM. The results showed that the mean height uncertainty decreased with each additional DEM that was added to the fusion process.

2.5.6 The maximum likelihood

The maximum likelihood method maximizes the probability associated with the estimated value of a pixel in the fused DEM. The errors between the fused DEM and Global Navigation Satellite System (GNSS) checkpoints were lower for the maximum likelihood (Ye et al., 2003; Eineder & Holzner, 2000; Eineder & Adam, 2005). Another application of maximum likelihood was in the work of (Jiang et al., 2014) where the variance of phase noise and the height of ambiguity were used for optimally determining the fusion weights. In this study fusion with maximum likelihood method was used due to having high accuracy in combining DEMs by considering their performance in eight different terrain types.

2.6 Vertical Accuracy Assessment

Similar to the accuracy assessment procedures implemented by (Gesch et al. 2012), vertical accuracies of the three DEMs were assessed by comparing the DEM elevations with those of the GCPs. At each point, the DEM elevations were extracted using Golden Surfer software. Then, the differences in elevation were computed by subtracting the GCP elevation from its corresponding DEM elevations, and these differences are the measured errors in the DEMs. For a particular DEM, positive errors represent locations where the DEM was above the GCP elevation, and negative errors occur at locations where the DEM was below the control point elevation. From these measured errors, the mean error and RMS for each DEM were calculated,

including standard deviations of the mean errors. The mean error (or bias) indicates if a DEM has an overall vertical offset (either positive or negative) from true ground level (Gesch et al., 2012). Finally, accuracy assessment results were analyzed by land-cover types to look for relationships between vertical accuracy and cover type.

CHAPTER THREE

METHODOLOGY

This research is concerned with the vertical assessment of fused DEM from ASTER-1″, COPERNICUS-1″, NASADEM-1″ & SRTM-1″-v3 public GDEMs using GPS Ground Controls in Tanzania. The first stage assesses involvement of the performance of the four Public Global DEMs in each a particular type of terrain and land cover at a national scale by considering available GPS Ground Control Points. After knowing the performance of each selected Public GDEMs in a particular type of terrain and land cover then, fusion was performed by taking the Public Global DEM having best performance in each particular type of terrain, then the fused DEM was generated. Since the Global assessment cannot indicate the limitations of DEMs due to their acquisition mode for example in rugged regions the SAR interferometry used to construct the DEM may fail due to the radar backscatter is disrupted in mountainous areas, we could expect DEM inconsistencies in such regions (Satge, 2014). Thus, in this research eight different types of terrain and land covers are considered in the assessment of the vertical performance of the four Public GDEMs. The elevations of Public GDEMs and GGCPs were converted into a uniform vertical datum (VD) i.e. EGM96 Global Geoid Model.

3.1 The procedures that used in vertical assessment of fused DEM from GDEMs using GPS Ground Controls

This research is concerned with the vertical assessment of fused DEM from ASTER-1″, COPERNICUS-1″, NASADEM-1″ & SRTM-1″-v3 public GDEMs using GPS Ground Controls in Tanzania. The procedures that used to determine the vertical assessment of fused DEM from Global Digital Elevation Models using GPS Ground Control Points in Tanzania are explained as follow.

3.1.1 The distinct areas selected for comparison, performance assessment and validation of GDEMs in Tanzania before fusion

Eight areas were chosen based on two main criteria: (1) the nature of terrain, and (2) the diversity of the land cover and relief, as these are the main factors known to influence DEM accuracy. This study area was chosen where a reference model was freely available and where different topographic conditions (flat, hilly, and mountainous areas) existed with various land cover types. Eight areas were chosen in this research are flat and bare terrain, mountainous and forested area, forested and fairly flat terrain, flat and plain terrain, highlands and forested

terrain, slightly mountainous and forested area, flat and forested coastal low land terrain, barely flat and forested coastal terrain.

i. Flat and bare terrain

The selected area is located in Dodoma region ranges between 5.3°S-6.92°S latitudes and 35.6°E-37.4°E longitudes respectively.

Figure 2: 3D view of flat and bare terrain in Dodoma

ii. Mountainous and forested area

The selected area is in kilimanjaro and Arusha regions which ranges between 2.36°S-4.2°S latitudes and 36.3°E-38.42°E longitudes respectively.

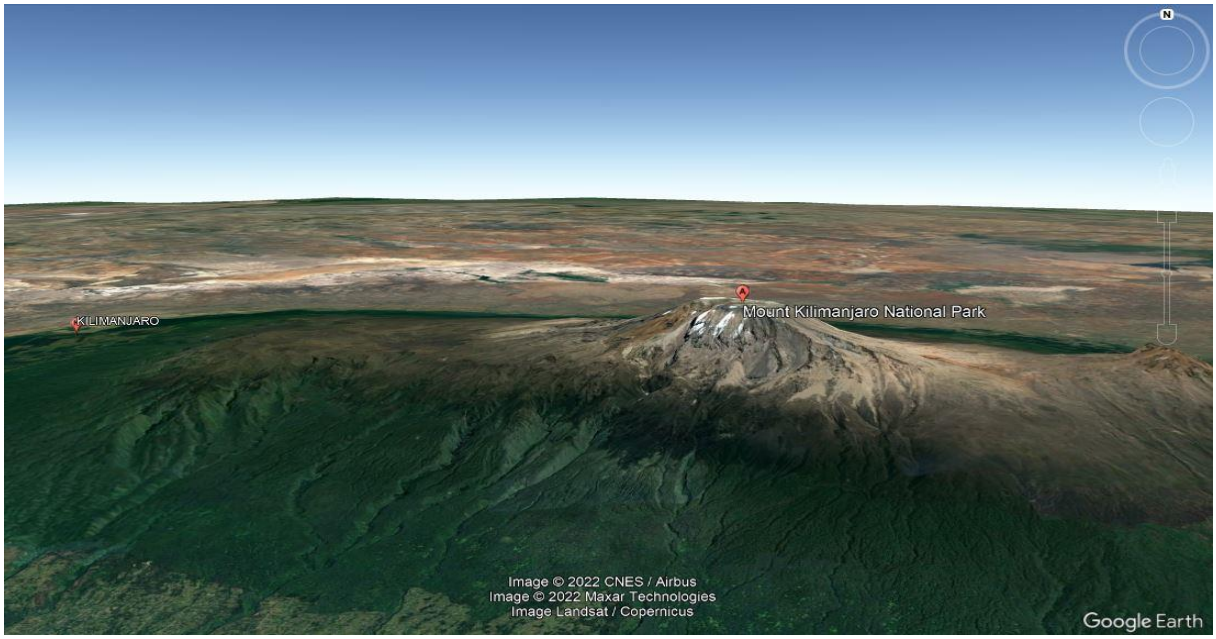

Figure 3: 3D view of a mountainous and forested area in Kilimanjaro and Arusha

iii. Forested and fairly flat terrain

The selected area is located in Tanga ranges between 4.16°S-5.48°S latitudes and 37.72°E-39.30°E longitudes respectively.

Figure 4: 3D view of a forested and fairly terrain in Tanga

iv. Flat and plain terrain

The selected area is in Tabora region ranges within 4°S-7°S latitudes and 31°E-34°E longitudes respectively.

Figure 5: 3D view of a flat and plain terrain in Tabora

v. Highlands and forested terrain.

The selected area is located in Mbeya region ranges between 7.59°S-9.02°S latitudes and 33.27°E-35.08°E longitudes respectively.

Figure 6: 3D view of highland and forested area in Mbeya

vi. Slightly mountainous and forested area.

The selected area is found in Morogoro region lies between 5.967°S-9.98°S latitudes and 35.42°E-37.11°E longitudes respectively.

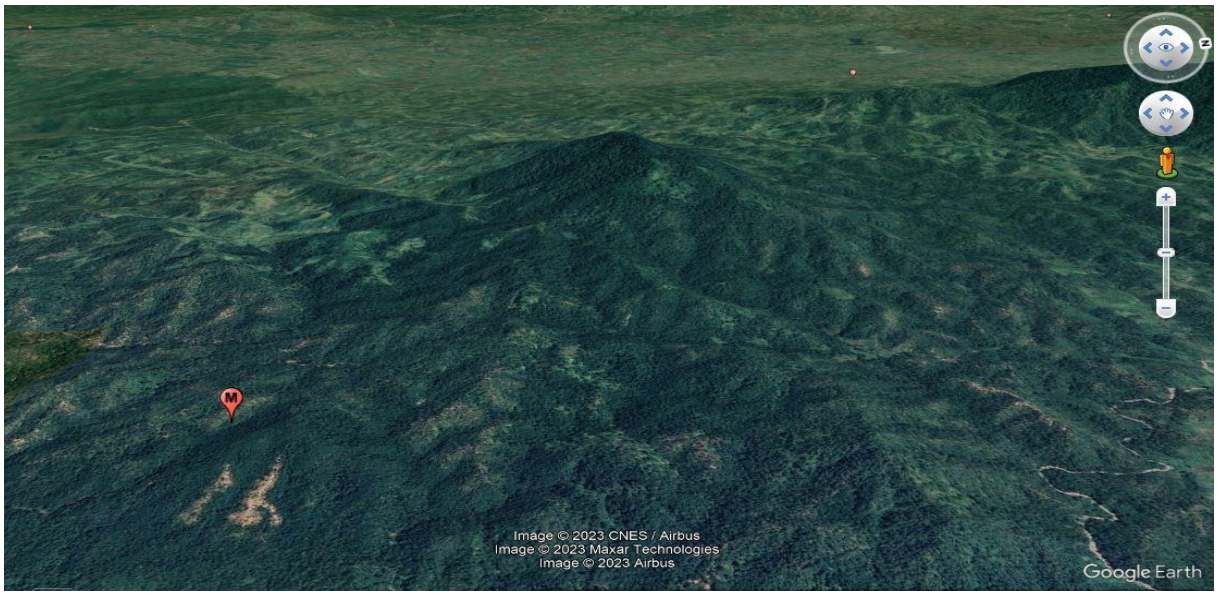

Figure 7: 3D view of Slightly mountainous and forested area in Morogoro

vii. Flat and forested coastal low land terrain.

The selected area in this part is Lind region which ranges from 8°S-11°S latitudes and 37°E-40°E longitudes respectively.

Figure 8: 3D view of Flat and forested coastal low land terrain in Lindi

viii. Barely flat and forested coastal terrain

The selected area is located in Mtwara region which ranges between 10°S-12°S latitudes and 38°E-41°E longitudes respectively.

Figure 9: 3D view of Barely flat and forested coastal terrain in Mtwara.

3.1.2 Conversion of GGCPs Ellipsoidal Heights to EGM96 Orthometric Heights

The process of converting GGCPs orthometric heights based on WGS84 to EGM96 orthometric heights involves subtracting the EGM96 geoid height from the GGCPs ellipsoidal height based on WGS84 as shown below.

$$H_{EGM96}^{GGCPs} = h_{WGS84}^{GGCPs} - N_{EGM96} \quad \text{..... 3.1}$$

Where;

h_{WGS84}^{GGCPs} is the ellipsoidal height from GPS measurements.

H_{EGM96}^{GGCPs} is the orthometric heights based on EGM96.

N_{EGM96} is the geoid heights based on EGM96.

Also, the Orthometric height of COPERNICUS-1″, ASTER-1″ and SRTM-1″ based on their Vertical Datum were converted into Orthometric height based on EGM96. NASADEM-1″ remain unchanged because it has orthometric height based on EGM96.

$$H_{VD}^{GDEM} = h_{VD}^{GDEM} - N_{VD} \quad \text{..... 3.2}$$

Where;

h_{VD}^{GDEM} is the ellipsoidal height from the respective GDEM based on its Vertical Datum.

H_{VD}^{GDEM} is the Orthometric height from respective GDEM based on its Vertical Datum.

N_{VD} is the Geoidal height based on Vertical Datum (VD).

3.1.3 Fusion of Public GDEMs

The fusion was done by taking DEM which has lower RMS which obtained from statistical of height difference between DEMs and GPS Ground Controls Points in each a particular type of terrain and land covers and input them in the software known as Global Mapper through data fusion (Mosaic) then the fused DEM was generated. This fusion method known as maximum likelihood method.

The following are the criteria to be considered during the fusion.

The present work is built according the following crucial assumption:

- The input DEM should in raster or grid format.
- The input DEMs should have similar vertical datum.
- The input DEMs should have similar resolution.
- The input DEMs should contain coinciding grid points (100% overlapping), which means either the input grids are identical or that the resolution of one DEM is an integer of the resolution of the other DEM.

To perform the fusion of input DEMs, the following procedures below should be followed.

Global Mapper: File > Open data File > select required data> view > contents for raster properties

- To generate fused DEM**,** right click the loaded data > Layer > Export > Select export format> Surfer Grid Export Option > Select OK.

3.1.4 Extraction of heights from Golden Surfer Software

Heights extracted from fused DEM and GDEMs using Golden Surfer software on the area of interest with respect to GGCPs Height data. Procedures for Extraction of heights is as shown below;

Golden Surfer 16: Grids > residuals > input Grid file (DEM)> input xyz data (control points in .csv format) > define data columns > OK

3.1.5 Validation of the fused DEMs using GPS Ground Control Points

Validation was done by comparing the GPS orthometric heights at 593 locations to the corresponding orthometric heights of fused DEM and GDEMs at respective GPS positions. Elevation of the fused DEM and GDEM at 593 locations computed by using Surfer 16 grid-residual module. The following bellow is the mathematical relation used to validate the orthometric heights of the fused DEMs and GDEMs with corresponding the orthometric heights of GGCPs within the area of interest (AOI).

$$\Delta H_i^{GGCPs,DEM} = H_i^{GGCPs} - H_i^{DEM} \quad \text{..... 3.3}$$

Where;

$\Delta H_i^{GGCPs,DEM}$ is the height differences between GPS Ground Control Points and DEM at location *i*.

H_i^{GGCPs} is the orthometric height from GPS Ground Control Points at location *i*.

H_i^{DEM} is the orthometric height from respective DEM at location *i*.

3.1.6 Comparison of the fused DEM and four GDEMs in Countrywide.

This part involves the process of comparing fused DEM with four selected Public GDEMs, the comparison is done by subtracting the elevations between the fused DEM and Public GDEMs at their grid intersections within Area of Interest (AOI).

$$\Delta H_i^{FDEM,GDEM} = H_i^{FDEM} - H_i^{GDEM} \quad \text{..... 3.4}$$

Where;

$\Delta H_i^{FDEM,GDEM}$ is the difference in elevation between the fused DEM and GDEM at their grid intersections.

H_i^{FDEM} and H_i^{GDEM} are the Fused DEM and GDEM elevations for COPERNICUS-1″, ASTER-1″, NASADEM-1″ and SRTM-1″respectively at their grid intersections within the area of interest.

3.1.7 Statistical assessment of height differences between fused DEM and GGCPs within the (AOI).

There are several methods that are used to assess the height differences between fused DEM and GPS Ground Control Points, includes Standard Deviation (SD), Root Mean Square(RMS) or Mean Absolute Error (MAE) as measures of the overall accuracy of the fused DEM. The measures provide a numerical estimate of the difference between the elevation values of the FDEM and GPS Ground Control Points. The performance of the fused DEM is obtained from the computed statistics of the difference between the elevation values of the fused DEM and GPS Ground Control Points.

a) Standard Deviation (SD) of height differences between GGCPs and Fused DEM.

$$\sigma_i = \pm\sqrt{\frac{\sum_{i=1}^{N}\left(\Delta H_i^{GGCPs,FDEM} - \Delta H_{mean}\right)^2}{N-1}} \quad \ldots\ldots\ldots\ldots\ldots\ldots\ldots\ldots\ldots\ldots\ldots\ldots \; 3.5$$

a) Root Mean Square(RMS) of the height differences between GGCPs and Fused DEM.

$$RMS = \pm\sqrt{\frac{\sum_{i=1}^{N}\left(\Delta H_i^{GGCPs,FDEM}\right)^2}{N}} \quad \ldots\ldots\ldots\ldots\ldots\ldots\ldots\ldots\ldots\ldots\ldots\ldots\ldots\ldots\ldots\ldots \; 3.6$$

a) Mean Absolute Error (MAE) between the GGCPs and Fused DEM.

$$\Delta H_{mean} = \frac{1}{N}\sum_{i=1}^{N}\Delta H_i^{GGCPs,FDEM} \quad \ldots\ldots\ldots\ldots\ldots\ldots\ldots\ldots\ldots\ldots\ldots\ldots\ldots\ldots\ldots\ldots \; 3.7$$

Where:

N is the number of GGCPs that are used.

$\Delta H_i^{GGCPs,FDEM}$ is the difference in elevation between the fused DEM and GPS Ground Control Points at location *i*.

3.2 Data requirement, preparation and management

In this study GPS Ground Controls, COPERNICUS-1″, ASTER-1″, NASADEM-1″, SRTM-1″, EGM08 and EGM96 were required. All data are available online except GPS Ground Controls and are downloaded from archives, official web sites of owners of the data as shown on (Table3.1).

Table 3.1: shows the websites used for accessing online data

S/N	DATA	WEB SITES
1	EGM08 & EGM96	http://164.214.2.53/GandG/wgs84/gravitymod/egm96/egm96.html
2	NASADEM-1″	https://portal.opentopography.org
3	COPERNICUS-1″	https://portal.opentopography.org
4	ASTER-1″	https://lpdaac.usgs.gov/tools/earthdata
5	SRTM-1″	https://lpdaac.usgs.gov/tools/earthdata

GPS ground control points (GCPs) are locations on the Earth's surface that have known coordinates (latitude, longitude, and elevation) that are determined using GPS measurements. In this study GPS ground control points are used to "ground truth" or validate the accuracy of the fused DEM created from COPERNICUS DEM and SRTM DEM. 594 Ground Control Points (GCPs) were used for the vertical performance assessment of the fused DEM, their positions are described by ellipsoidal curvilinear coordinates (φ, λ) determined using Global Positioning System (GPS) and orthometric heights (H) over Tanzania. By comparing the elevations of the GGCPs to the elevations of the same locations in the DEMs, we can assess the "vertical performance" of the fused DEM and determine how well they match reality.

EGM08 and EGM96 are the models of the Earth's gravity field, in this study EGM08 and EGM96 were used to convert ellipsoidal heights (measured from the Earths ellipsoidal surface) to orthometric heights (measured from the Earths geoid, which represents mean sea level). The conversion process is called orthometric height correction or geoid height correction, and it require the use of geoid models such as EGM08 and EGM96.

The SRTM-30m and ASTER GDEMs were both downloaded from LP DAAC Global Data Explorer (http://gdex.cr.usgs.gov/gdex/), in GeoTIFF format with Universal Transverse Mercator projection and the World Geodetic System (WGS) 1984 as horizontal datum. They both have the Earth Gravitational Model 1996 (EGM96) as vertical datum.

The NASADEM (released in February 2020) was created by reprocessing of the SRTM radar data, and merging it with other DEM datasets, such as ASTER, ICESat and GLAS. The main objective was to eliminate voids and other limitations that were present in the SRTM dataset. The NASADEM is supposed to be the successor of the SRTM DEM dataset. In our study, we used the NASADEM dataset that was released in February 2020.

The Copernicus DEM is a Digital Surface Model (DSM) that represents the Earth's surface, including buildings, infrastructure, and vegetation. It is derived from an edited DSM called World DEM, which includes adjustments for water bodies, river flow, shorelines, coastlines, airports, and unrealistic terrain structures. The World DEM is based on radar satellite data from the TanDEM-X Mission, funded by a partnership between the German State (represented by DLR) and Airbus Defense and Space.

Open Topography provides access to the global 30m (GLO-30) DSM through a public AWS S3 bucket established by Sinergise. The original datasets have varying cell spacing based on latitude, but Open Topography resamples the data north of 50 degrees' latitude and south of -

50 degrees latitude to maintain consistent pixel dimensions of 30m or 90m for data accessed through their web interface or API. The Copernicus 30m dataset is referenced to the horizontal datum WGS84 and the vertical datum EGM2008.

3.3 Software used

The following below are the software's that are used in this research.

i. Global Mapper Pro

This software was used to open and convert the selected Public GDEMs from GEOTIFF format to Surfer Grid (Binary v7 Format) for further processing in Golden Surfer software, also it was used in the fusion of FUSED DEM.

ii. Golden Surfer v16

This software is used to convert the public GDEMs from surfer grid format to DAT format (XYZ) for elevations extraction and other grid data manipulation, also to acquire the height information from intersection points of the fused DEM, Public GDEM and GGCPs by residual computation and finally to compute the height differences between the fused DEM and selected Public GDEMs, also to compute required statistics.

iii. ArcMap version 10.7

This software is used to prepare a map shows the distribution of GPS Ground Control Points in the area of interest.

iv. Microsoft Excel

This sheet is used to prepare tables results and to compute Root Mean Square from height differences between fused DEM and GPS Ground Controls Points.

v. Microsoft word

This was used to prepare research report.

CHAPTER FOUR

RESULTS, ANALYSIS AND DISCUSION

3.1 RESULTS

Statistics of height differences between the fused DEM vs GGCPs and four GDEMs vs GGCPs in eight selected types of terrain and land covers, also statistics of height differences between the Fused DEM vs GGCPs and four GDEMs vs GGCPs countrywide are presented in this chapter. Statistics calculated consist of number of values, minimum, maximum, mean, standard deviation and Root Mean Square value.

For simplification the eight selected types of terrain and land covers are assigned the letters A1, A2, A3, A4, A5, A6, A7, and A8 as presented in Table-4.1.

Table 4.1: Shows the Symbols representing the 8 types of terrains and land covers.

Terrain and land covers	Description
A1	Flat and bare terrain (Dodoma)
A2	Mountainous and forested terrain (kilimanjaro and Arusha)
A3	Flat and forested terrain (Lindi)
A4	Highlands and forested terrain (Mbeya)
A5	Slightly mountainous and forested terrain (Morogoro)
A6	Barely flat and forested coastal terrain (Mtwara)
A7	Flat and plain terrain (Tabora)
A8	Flat and fairly flat terrain (Tanga)

3.1.1 The statistical difference between fused DEM, four GDEMs using GGCPs in eight representative terrain and land covers

The statistics of height difference between fused DEM vs GGCPs and four GDEMs vs GGCPs in eight representative terrain and land covers were computed using Equation 3.5, 3.6 and 3.7 and their results are presented in Table 4.2 to Table 4.9, as shown below.

Table 4.2: Shows the statistics of height difference between fused DEM vs GGCPs and four GDEMs vs GGCPs in A1.

STATISTICS							
GDEMs	N	SUM (m)	MIN (m)	MAX (m)	MEAN (m)	STD (m)	RMS (m)
COPERNICUS-30m	18	24.1	-0.6	3.0	1.3	0.9	1.6
NASADEM-30m	18	44.7	-0.8	5.7	2.5	1.5	2.9
ASTER-30m	18	-188.7	-17.7	-4.6	-10.5	3.8	11.1
SRTM-30m	18	-373.5	-24.4	16.4	-20.7	2.2	20.9
FUSED DEM	18	0.8	-1.7	2.1	0.05	1.1	1.1

Table 4.3: Shows the statistics of height difference between fused DEM vs GGCPs and four GDEMs vs GGCPs in A2.

STATISTICS							
GDEMs	N	SUM (m)	MIN (m)	MAX (m)	MEAN (m)	STD (m)	RMS (m)
COPERNICUS-30m	10	395.3	34.7	46.3	39.5	3.6	39.7
NASADEM-30m	10	402.1	31.1	50.1	40.2	6.5	40.7
ASTER-30m	10	303.5	23.3	35.9	30.3	4.1	30.6
SRTM-30m	10	205.7	13.2	30.1	20.6	5.3	21.2
FUSED DEM	10	198.4	9.0	40.8	19.8	8.7	21.5

Table 4.4: Shows the statistics of height difference between fused DEM vs GGCPs and four GDEMs vs GGCPs in A3.

STATISTICS							
GDEMs	N	SUM (m)	MIN (m)	MAX (m)	MEAN (m)	STD (m)	RMS (m)
COPERNICUS-30m	38	-62.6	-3.2	0.3	-1.6	0.9	1.9
NASADEM-30m	38	-57.9	-5.8	2.1	-1.5	1.9	2.4
ASTER-30m	38	-1048.8	-59.9	-6.1	-27.6	10.7	29.6
SRTM-30m	38	-1213.2	-39.6	-27.8	-31.9	2.3	32.0
FUSED DEM	38	-139.4	-7.7	-1.2	-3.7	1.4	3.9

Table 4.5: Shows the statistics of height difference between fused DEM vs GGCPs and four GDEMs vs GGCPs in A4.

STATISTICS							
GDEMs	N	SUM (m)	MIN (m)	MAX (m)	MEAN (m)	STD (m)	RMS (m)
COPERNICUS-30m	12	18.7	-0.1	3.5	1.6	1.0	1.8
NASADEM-30m	12	30.6	0.4	5.6	2.6	1.7	3.0
ASTER-30m	12	-163.1	-25.3	-4.2	-13.6	6.4	14.9
SRTM-30m	12	-200.0	-19.7	-12.0	-16.7	2.4	16.8
FUSED DEM	12	0.6	-3.8	1.8	0.1	1.6	1.5

Table 4.6: Shows the statistics of height difference between fused DEM vs GGCPs and four GDEMs vs GGCPs in A5.

STATISTICS							
GDEMs	N	SUM (m)	MIN (m)	MAX (m)	MEAN (m)	STD (m)	RMS (m)
COPERNICUS-30m	10	2.4	-2.3	4.5	0.2	1.9	1.9
NASADEM-30m	10	18.6	-3.3	7.6	1.9	3.1	3.5
ASTER-30m	10	-138.3	-22.9	3.1	-13.8	7.4	15.5
SRTM-30m	10	-240.5	-30.1	-16.7	-24.1	3.9	24.3
FUSED DEM	10	-17.4	-4.7	3.8	-1.7	2.5	2.9

Table 4.7: Shows the statistics of height difference between fused DEM vs GGCPs and four GDEMs vs GGCPs in A6.

STATISTICS							
GDEMs	N	SUM (m)	MIN (m)	MAX (m)	MEAN (m)	STD (m)	RMS (m)
COPERNICUS-30m	14	-35.0	-4.9	-0.3	-2.5	1.4	2.8
NASADEM-30m	14	-18.8	-5.8	3.1	-1.3	2.8	3.1
ASTER-30m	14	-392.7	-53.5	-14.5	-28.0	10.9	29.9
SRTM-30m	14	-433.0	-35.8	-25.7	-30.9	3.2	31.1
FUSED DEM	14	-65.2	-8.8	-1.6	-4.7	2.0	4.9

Table 4.8: Shows the statistics of height difference between fused DEM vs GGCPs and four GDEMs vs GGCPs in A7.

STATISTICS							
GDEMs	N	SUM (m)	MIN (m)	MAX (m)	MEAN (m)	STD (m)	RMS (m)
COPERNICUS-30m	47	-61.6	-6.3	3.0	-1.3	1.7	2.1
NASADEM-30m	47	-40.1	-5.4	4.4	-0.9	2.0	2.2
ASTER-30m	47	-1025.9	-41.4	-10.3	-21.8	5.6	22.5
SRTM-30m	47	-1019.7	-27.1	-14.1	-21.7	2.9	21.9
FUSED DEM	47	-134.8	-8.9	1.8	-2.9	2.0	3.5

Table 4.9: Shows the statistics of height difference between fused DEM vs GGCPs and four GDEMs vs GGCPs in A8.

STATISTICS							
GDEMs	N	SUM (m)	MIN (m)	MAX (m)	MEAN (m)	STD (m)	RMS (m)
COPERNICUS-30m	15	-6.7	-3.3	1.7	-0.4	1.4	1.5
NASADEM-30m	15	-9.1	-5.9	3.6	-0.6	2.9	2.9
ASTER-30m	15	-308.1	-43.3	-11.9	-20.5	8.4	22.1
SRTM-30m	15	-396.9	-36.1	-22.2	-26.5	4.4	26.8
FUSED DEM	15	-42.3	-12.6	0.1	-2.8	3.4	4.3

3.1.2 The statistics of height difference between fused DEM vs GGCPs and four GDEMs vs GGCPs countrywide

The statistics of height difference between fused DEM vs GGCPs and four GDEMs vs GGCPs over AOI were computed using equation 3.5, 3.6 and 3.7 and their results are presented in Table 4.10 as shown below.

Table 4.10: Shows the statistics of height difference between Fused DEM vs GGCPs and four GDEMs vs GGCPs countrywide.

STATISTICS	GGCPs vs FUSED DEM-90m	GGCPs vs COPERNICUS-90m	GGCPs vs NASADEM-90m	GGCPs vs ASTER-90m	GGCPs vs SRTM-90m
N	593	593	593	593	593
SUM	-520.6	-872.7	-520.6	-9473.3	-13573.3
MIN	-9.7	-11.5	-9.7	-69.3	-39.0
MAX	35.7	36.2	35.7	10.3	5.5
MEAN	-0.9	-1.5	-0.9	-15.9	-22.9
SD	3.5	3.2	3.5	8.9	6.3
RMS	12.2	3.6	3.6	18.3	23.7

3.1.3 The statistics of height difference between fused DEM and four selected public GDEMs Countrywide

The statistics of height difference between fused DEM and four selected public GDEMs countrywide were computed using Equation 3.5, 3.6 and 3.7, and the results are presented in Table 4.11 as shown below.

Table 4.11: Shows the statistics of height difference between fused DEM and four public GDEMs Countrywide.

STATISTICS	FUSED DEM vs COPERNICUS-90m	FUSED DEM vs NASADEM-90m	FUSED DEM vs ASTER-90m	FUSED DEM vs SRTM-90m
N	593	593	593	593
SUM	-2344.9	-1992.8	-10945.5	-15045.5
MIN	-41.2	-42.9	-67.3	-64.5
MAX	23.8	22.4	18.8	0.002
MEAN	-3.9	-3.4	-18.5	-25.4
SD	12.1	12.3	14.6	12.1
RMS	12.7	12.7	23.5	28.1

3.2 DISCUSSION OF RESULTS

The discussion of results is based on the value of the mean, SD and RMS statistics. The DEM with the least value of the mean, SD and RMS is the one which termed as the best DEM than the others, Mean is preferred because it takes to account all the values in the data set, hence the best estimator of the true value (Elkhrarchy, 2016). SD tells how accurate the mean of any given sample from that population is likely to be compared to the true population mean and RMS is used because the RMS is centered on zero such that the RMS measures the differences between the value of DEM Heights and the value of the reference data set elevation, and aggregates them to a single measure of predictive power (Dominicus, 2020). This research considered eight different types of terrains and land covers categorized as follows.

3.2.1 Performance of Public GDEMs in eight selected types of terrains and land covers

In eight selected types of terrains and land covers, Copernicus-30m shows better performance over SRTM-30m, ASTER-30m and NASADEM-30m in seven selected types of terrains and land covers, also SRTM-30m shows better performance over COPERNICUS-30m, ASTER-30m and NASADEM-30m for the left type of terrain and land covers. The results are discussed as follows.

a. Flat and bare terrain (Dodoma).

In Dodoma region, the results show that fused DEM has a better performance over Copernicus-30m, NASADEM-30m, ASTER-30m and SRTM-30m with RMS ±1.095, ±1.622m, ±2.887m, ±11.123m and ±20.859m respectively.

b. Mountainous and forested terrain (kilimanjaro and Arusha).

In Kilimanjaro and Arusha regions, the results show that SRTM-30m has a better performance over fused DEM-30m, NASADEM-30m, ASTER-30m and Copernicus-30m with RMS ±21.183m, ±21.483, ±40.683m, ±30.590m and ±39.671m respectively.

c. Flat and forested terrain (Lindi).

In Lindi region, the results show that Copernicus-30m has a better performance over fused DEM-30m, NASADEM-30m, ASTER-30m and SRTM-30m with RMS ±1.921m, ±3.907, ±2.440m, ±29.552m and ±32.009m respectively.

d. Highlands and forested terrain (Mbeya).

In Mbeya region, the results show that fused DEM-30m has a better performance over Copernicus-30m, NASADEM-30m, ASTER-30m and SRTM-30m with RMS ±1.496, ±1.848m, ±3.019m, ±14.923m and ±16.826m respectively.

e. Slightly mountainous and forested terrain (Morogoro).

In Morogoro region, the results show that Copernicus-30m has a better performance over fused DEM-30m, NASADEM-30m, ASTER-30m and SRTM-30m with RMS ±1.863m, ±2.913, ±3.460m, ±15.509m and ±24.329m respectively.

f. Barely flat and forested coastal terrain (Mtwara).

In Mtwara region, the results show that Copernicus-30m has a better performance over fused DEM-30m, NASADEM-30m, ASTER-30m and SRTM-30m with RMS ±2.847m, ±4.879, ±3.056m, ±29.960m and ±31.081m respectively.

g. Flat and plain terrain (Tabora).

In Tabora region, the results show that Copernicus-30m has a better performance over fused DEM-30m, NASADEM-30m, ASTER-30m and SRTM-30m with RMS ±2.132m, ±3.497, ±2.175m, ±22.519m and ±21.892m respectively.

h. Flat and fairly flat terrain (Tanga).

In Tanga region, the results show that Copernicus-30m has a better performance over fused DEM-30m, NASADEM-30m, ASTER-30m and SRTM-30m with RMS ±1.466m, ±4.297, ±2.863m, ±22.095m and ±26.803m respectively.

3.2.2 General Performance of Fused DEM with GDEMs in Tanzania

In Countrywide validation using GGCPs, the fused DEM-90m, shows better performance over SRTM-90m and ASTER-90m but not over COPERNICUS-90m and NASADEM-90m with RMS ±12.173m, ±23.726m, ±18.303m, ±3.552m and ±3.648m respectively.

CHAPTER FIVE

CONCLUSION AND RECOMMENDATION

3.3 Conclusion

From Table-4.10, the results show that the general vertical performance of fused DEM as assessed from GPS Ground Control Points Countrywide is superior to SRTM-90m and ASTER-90m based on the smallest value of RMS which is ±12.173m, ±23.726m, ±18.303m respectively. Also the fused DEM is inferior to COPERNICUS-90m and NASADEM-90m with RMS ±12.173m, ±3.552m and ±3.648m respectively. Also in eight selected terrain and land covers the performance of fused DEM varies from one place to another because of different factors such as terrain complexity such as Steep mountains, valleys, water bodies, or dense vegetation can pose challenges for data acquisition and processing, potentially leading to reduced accuracy in these areas and also the algorithms used for data fusion can also contribute to performance variation, some regions might be better suited to specific fusion methods as a resulting in more accurate results while others may be more challenging and yield less accurate outputs and the results show that fused DEM has better performance in Flat and bare terrain (Dodoma) and Highlands and forested terrain (Mbeya) over Copernicus, SRTM, ASTER and NASADEM, while in other terrain and land covers the fused DEM is inferior for some selected GDEMs based on particular terrain and land cover. Therefore, it is suggested that fused DEM can be used for any application depending upon the accuracy demand.

3.4 Recommendation

It is recommended that further fusion of Global Digital Elevation Models should be continued by considered other fusion methods, current Digital Elevation Models like FABDEM and more than eight types of terrains and land covers. In addition, the assessment of vertical performance of fused DEM should continue using topographic map.

REFERENCES

Abrams, M., Hook, S., Ramachandran, B., & Fraser, R. (2002). The ASTER global digital elevation model and ASTER sensor complement. *In Geoscience and Remote Sensing Symposium (IGARSS). 2002 IEEE International, Vol. 3,* , pp. 1514-1516.

Aguilar, F.J., Agüera, F., Aguilar, M.A., & Carvajal, F. (2005). Effects of Terrain Morphology, Sampling Density, and Interpolation Methods on Grid DEM Accuracy. *Photogrammetric Engineering & Remote Sensing,*, 71 (7), 805–816.

Astrium. (2013). *WorldDEM.* Retrieved on June 12, 2013, from http://www.astrium-geo.com/worlddem/

Azzaro, R. B. (2012). The volcano -tectonic map of Etna volcano, 1:100.000 scale: an intergrated approach based on a morphotectonic analysis from high-resolution DEM constrained by geologic, active faulting and seismotectonic data. *Ital. J. Geosci.*, 131, 153-170. Retrieved from https:/doi.org/10.3301/Ijg.2011.29.

Bamler, R. and Hartl, P. (1998). Synthetic aperture radar interferometry. *Inverse Problems,*, 14, R1-R54.

Bater, C.W., & Coops, N.C. (2009). Evaluating error associated with lidar-derived DEM interpolation. *Computers and Geosciences*,, 35, 289 – 300.

Bortolota, Z.J., & Wynne, R.H. (2005). Estimating forest biomass using small footprint LiDAR data: An individual tree-based approach that incorporates training data. *ISPRS Journal of Photogrammetry & Remote Sensing,* , 59, 342– 360.

Coveney, S., & Fotheringham, A.S. (2011). Terrestrial Laser Scan Error in the Presence of Dense Ground Vegetation. *The Photogrammetric Record,*, 26(135), 307–324.

Crosetto, M., & Aragues, F. P. (2000). Radargrammetry and SAR interferometry for DEM generation: Validation and data fusion. *CEOS SAR Workshop,*, 450, 367-372.

Denker, H. (2005). Evaluation of SRTM3 and GTOPO30 terrain data in Germany. *In Gravity, Geoid and Space Missions*, (pp. 218-223).

Desmet, P. (1997). Effects of Interpolation Errors on the Analysis of DEMs. *Earth Surface Processes and Landforms,*, 22, 563-580.

Dobson, M. C., & Ulaby, F. T. (1986). Active microwave soil moisture research. *IEEE Transactions on Geoscience and Remote Sensing,*, 1, 23-36.

Dominicus, E. (2020). *Vertical Accuracy Assessment and Comparison of ALOSV2.2-1" AND TanDEM-X-3" Using Ground Control Points in Tanzania.* Dar es Salaam: a B.Sc. Disertation Department of Geomatics, SGST, Ardhi University, Tanzania.

Eineder, M. & Adam, N. (2005). A maximum-likelihood estimator to simultaneously unwrap, geocode, and fuse SAR interferograms from different viewing geometries into one Digital Elevation Model. *IEEE Transactions on Geoscience and Remote Sensing*, 43(1), 24–36.

Eineder, M. & Holzner, J. (2000). Interferometric DEMs in alpine terrain-limits and options for ERS and SRTM. *In Proc. IEEE IGARSS.*

Elkhrachy, I. (2018). Vertical accuracy assessment of SRTM and ASTER Digital Elevation Models: A case study of Najran city, Saudi Arabia. *Ain Shams Engineeing Journal*, 9(4),1807-1817. Retrieved from https://doi.org/10.1016/J.ASEJ.2017.01.007

Elkhrarchy, I. (2016). Vertical accuracy asessment of SRTM and ASTER Digital Elevation Models. *Ain shams Engineering journal* , pp 1807-1817.

Farr T. & Kobrick M. (2001.). The Shuttle Radar Topography Mission, Eos Trans. *American Geophysical Union,*, 82 (47), 2001.

Farr, T. (2007). The Shuttle Radar Topography Mission. *Reviews of Geophysics*, 45(2). doi:doi: 10.1029/2005RG000183

Fayard, F., Méric, S., & Pottier, E. (2007). Matching stereoscopic SAR images for radargrammetric applications. *In IEEE International Geoscience and Remote Sensing Symposium, 2007, IGARSS 2007,*, 4364-4367.

Fisher, P.F. & Tate, N.J. (2006). Causes and consequences of error in digital elevation models. *Progress in Physical Geography*, 30(4), 467–489.

Gao, J. (2007). Towards accurate determination of surface height using modern geoinformatic methods:. *Progress in Physical Geography*, 31(6), 591–605.

Gesch, D., Oimoen, M., Zhang, Z., Meyer, D., & Danielson, J. (2012). Validation of the ASTER global digital elevation model version 2 over the conterminous United States. *In: The*

Inter-national Archives of the Photogrammetry, Remote Sensing and Spatial Information Sciences,, Vol. XXXIX-B4,, pp. 281-286.

Hastings, D. A., & Dunbar, P. K. (1998). Development & assessment of the Global Land One-km Base Elevation digital elevation model (GLOBE). *In: Fritsch, D., Englich, M., and Sester, M. (eds), ISPRS Commission IV Symposium on GIS – Between Vision and Applications, Stuttgart, Germany,*, 32(4), 218-221.

Hirt, C., Filmer, M. S., & Featherstone, W. E. (2010). Comparison and validation of the recent freely available ASTER-GDEM ver1, SRTM ver4. 1 and GEODATA DEM-9S ver3 digital elevation models over Australia. *Australian Journal of Earth Sciences,*, 57(3), 337-347.

Honikel, M. (1998). Fusion of optical and radar digital elevation models in the spatial frequency domain. *Second International Workshop on Retrieval of Bio- & Geo-Physical Parameters from SAR Data for Land Applications,* , 441, 537-543.

Hopkinson, C. & Demuth, M.N. (2006). Using airborne lidar to assess the influence of glacier downwasting on water resources in the Canadian Rocky Mountains. *Canadian Journal of Remote Sensing,*, 32(2), 212-222.

Hopkinson, C. (2006). An Overview of Airborne Laser Scanning Technology. In: Hydroscan – Airborne laser mapping of hydrological features and resources, edited by: Hopkinson, C., Pietroniro, A. and Pomeroy, J.W. *HYDROSCAN 2006 Proceedings,*, 7-22.

Jiang, H., Zhang, L., Wang, Y., & Liao, M. (2014). Fusion of high-resolution DEMs derived from COSMO-SkyMed and TerraSAR-X InSAR datasets. *Journal of Geodesy*, 88(6), 587–599. Retrieved from https://doi.org/10.1007/s00190-014-0708-x

Karkee, M., Steward, B. L., & Aziz, S. A. (2008). Improving quality of public domain digital elevation models through data fusion. *Biosystems Engineering,*, 101(3), 293-305.

Li, Z., G. Liu, & Ding, X. (2006). Exploring the Generation of Digital Elevation Models from Same-side ERS SAR Images: Topographic and Temporal Effects. *The Photogrammetric Record,*, 21(114), 124–140.

Lillesand, T.M., Kiefer, R.W., & Chipman, J.W. (2008). Remote Sensing and Image Interpretation (6th Ed.). *John Wiley and Sons, Inc.*, USA. 756 p.

Lindsay, J. (2006). Sensitivity of channel mapping techniques to uncertainty in digital elevation data. . *International Journal of Geographical Information Science*, , 20(6), 669–692.

Madsen, S.N., Zebker, H.A., & Martin, J. (1993). Topographic Mapping Using Radar Interferometry: Processing Techniques. *IEEE Transactions on Geoscience and Remote Sensing,*, 31(1), 246-256.

Mapunda, S. B. (2019). *Comparison and Vertical Performance Assessment of SRTM-1-v3, ALOS-1-v2, MERIT-3 and TanDEM-X-3 Public Global DEMs in Tanzania Using GPS Ground Controls.* Dar es Salaam: a B.Sc. Dissertation of the Department of Geomatics, SGST, Ardhi University, Tanzania.

Miliaresis, G. C., & Argialas, D. P. (2002). Quantitative representation of mountain objects extracted from the global digital elevation model (GTOPO30). *International Journal of Remote Sensing,*, 23(5), 949-964.

Milledge, D. G., Lane, S. N., & Warburton, J. (2009a). Optimization of Stereo-matching Algorithms Using Existing DEM Data. *Photogrammetric Engineering and Remote Sensing,*, 75(3), 323-333.

Nico, G., Leva, D., Antonello, G., & Tarchi, D. (2004). Ground-Based SAR Interferometry for Terrain Mapping: Theory and Sensitivity Analysis. *IEEE Transactions on Geoscience and Remote Sensing,*, 42(6), 1344-1350.

Nico, G., Leva, D., Antonello, G., Fortuny-Guasch, J., & Tarchi, D. (2005). Generation of Digital Terrain Models With a Ground-Based SAR System. *IEEE Transactions on Geoscience and Remote Sensing,*, 43(1), 45-49.

Ostrowski, J., & Cheng, P. (2002). DEM extraction from stereo SAR satellite imagery. *In Proceedings of the International Geoscience and Remote Sensing Symposium, 2000. IGARSS 2000.,*, 5, 2176-2178.

Paillou, P., & Gelautz, M. (1999). Relief reconstruction from SAR stereo pairs: the “optimal gradient” matching method. *IEEE Transactions on Geoscience and Remote Sensing,*, 37(4), 2099-2107.

Papasaika, H., Kokiopoulou, E., Baltsavias, E., Schindler, K., & Kressner, D. (2011). Fusion of digital elevation models using sparse representations. *Photogrammetric Image Analysis,*, 6952, 171-184.

Papasaika, H., Poli, D., & Baltsavias, E. (2009). Fusion of digital elevation models from various data sources. *In International Conference on Advanced Geographic Information Systems & Web Services,2009. GEOWS'09. IEEE.*, 117-122.

Poon, J., Fraser, C.S., Chunsun, Z., Li, Z. & Gruen, A. (2005.). Quality Assessment of Digital Surface. *The Photogrammetric Record,*, 20(110), 162-171.

Rabus, B., Eineder, M., Roth, A., & Bamler, R. (2003). The shuttle radar topography mission - a new class of digital elevation models acquired by spaceborne radar. *ISPRS Journal of Photogrammetry and Remote Sensing,*, 57(4), 241-262.

Reinartz, P., Müller, R., Hoja, D., Lehner, M., & Schroeder, M. (2005). Comparison and fusion of DEM derived from SPOT-5 HRS and SRTM data and estimation of forest heights. *Proc. EARSeL Workshop on 3D-Remote Sensing, Porto, June*, 9(3) 102-120.

Reuter, H. I., Nelson, A., Strobl, P., Mehl, W., & Jarvis, A. (2009). A first assessment of Aster GDEM tiles for absolute accuracy, relative accuracy and terrain parameters. *In IEEE International Geoscience and Remote Sensing Symposium, IGARSS 2009*, 21(5), 240 – 243.

Rishikeshan, C., Katiyar, S., Mahesh, V.V. (2014.). Detailed evaluation of DEM interpolation methods in GIS using DGPS data. *International Conference on Computational Intelligence and Communication Networks.*, IEEE,pp. 666-671. Retrieved from https://doi.org/10.1109/CICN.2014.148

Rosen, P.A., Hensley, S., Joughin, I.R., Li, F.K., Madsen, S.N., Rodriguez, E. & Goldstein, R.M. (2000). Synthetic Aperture Radar Interferometry. *Proceedings of the IEEE,*, 88(3), 333-382.

Roth, A., Knopfle, W., Strunz, G., Lehner, M., & Reinartz, P. (2002). Towards a global elevation product: Combination of multi-source digital elevation models. *International Archives of Photogrammetry Remote Sensing and Spatial Information Sciences,*, 34(4), 675-679.

Satge, F. B. (2014). Accuracy assessment of SRTM v4 and ASTER GDEM v2 over the Altiplano watershed using ICESat/GLAS data. *International Journal of Remote Sensing*, 36(2), pp.465-488.

Schultz, H., Hanson, A. R., Riseman, E. M., Stolle, F. R., Zhu, Z., & Dong-Min, W. (2002). A self-consistency technique for fusing 3d information. *In Proceedings of the Fifth IEEE International Conference on Information Fusion,*, 2, 1106-1112.

Schultz, H., Riseman, E. M., Stolle, F. R., & Woo, D. (1999). Error detection and DEM fusion using self-consistency., 1999. *In Proceedings of the Seventh IEEE International Conference on Computer Vision,*, 2, 1174-1181.

Slatton, K. C., Crawford, M., & Teng, L. (2002). Multiscale fusion of INSAR data for improved topographic mapping. *In IEEE International Geoscience and Remote Sensing Symposium, 2002. IGARSS'02.*, 1, 69-71.

Smith, L. (2002). Emerging Applications of Interf erometric Synthetic Aperture Radar (InSAR) in Geomorphology and Hydrology. *Annals of the Association of American Geographers,*, 92(3), 385-398.

Stilla, U., Soergel, U., & Thoennessen, U. (2003). Potential and limits of InSAR data for building reconstruction in built-up areas. *ISPRS Journal of Photogrammetry and Remote Sensing,*, 58(1), 113-123.

Tachikawa T., Hato M., Kaku M., & Iwasaki, A. (2011). Aster Global Digital Model Version 2- summary of validation results. *In Geoscience and Remote Sensing (IGARSS), 2011 IEEE International*, PP. 3657-3660.

Toutin, T. (1998). Stereo RADARSAT for mapping applications. . *In ADRO, Final Symposium. Montreal, Canada, ADRO (Vol. 453).*

Toutin, T. (2004). DSM generation and evaluation from QuickBird stereo imagery with 3D physical. *International Journal of Remote Sensing,*, 25(22), 5181-5193.

Toutin, T., & Chénier, R. (2009). 3-D Radargrammetric Modeling of RADARSAT-2 Ultrafine Mode: Preliminary Results of the Geometric Calibration. *IEEE Geoscience and Remote Sensing Letters,*, 6(2), 282-286.

Toutin, T., & Gray, L. (2000). Review: State-of-the-art of elevation extraction from satellite SAR data. *ISPRS Journal of Photogrammetry & Remote Sensing,*, 55, 13-33.

Toutin, T., Zakharov, I., & Schmitt, C. (2010). Fusion of Radarsat-2 polarimetric images for improved stereo-radargrammetric DEM. *International Journal of Image and Data Fusion,*, 1 (1), 67-82.

Townsend, P. A. (2002). Relationships between forest structure and the detection of flood inundation in forested wetlands using C-band SAR. . *International Journal of Remote Sensing,* , 23(3), 443-460.

Wechsler, S. (2007). Uncertainties associated with digital elevation models for hydrologic applications: a review. *Hydrology and Earth System Sciences,* , 11, 1481–1500.

Wehr, A., & Lohr, U. (1999). Airborne laser scanning - an introduction and overview. *ISPRS Journal of Photogrammetry and Remote Sensing,*, 54(2-3), 68-82.

Wulder, M. A., Bater, C. W., Coops, N. C., Hilker, T., & White, J. C. (2008). The role of LiDAR in sustainable forest management. *The Forestry Chronicle,*, 84(6), 807-826.

Ye, C. S., , Jeon, B. M., & Lee, K. H. (2003). Digital elevation model combination using triangular image warping interpolation and maximum likelihood. *Journal International Journal of Remote Sensing*, 24(18), 3683–3689.

Zebker, H. A., & Villasenor, J. (1992). Decorrelation in interferometric radar echoes. *IEEE Transactions on Geoscience and Remote Sensing,*, 30(5), 950-959.

APPENDIX

GPS GROUND CONTROL POINTS OVER 593 STATIONS IN TANZANIA			
LONGITUDE	LATITUDE	H (m)	H_EGM96 (m)
34.80028	-11.2737	540.151	541.7149
37.34053	-11.0626	693.8507	692.5481
40.18494	-10.3347	110.619	109.373
35.75316	-7.67593	1428.14	1430.789
31.60572	-7.95119	1801.63	1806.146
39.11663	-5.08776	9.863	9.631397
32.82546	-5.04023	1218.3	1216.865
29.66836	-4.88672	821.835	821.5257
31.79922	-1.32555	1251.396	1249.908
32.92252	-2.447	1144.671	1143.28
33.83795	-1.53753	1184.789	1183.532
37.80493	-6.74847	502.114	502.9354
32.82546	-5.04015	1222.85	1221.415
37.3371	-3.34995	858.603	861.4496
39.20793	-6.76559	97.461	97.23851
39.29718	-6.81781	50.396	50.13307
39.21072	-6.21853	24.024	23.68102
35.7483	-6.16964	1119.971	1120.901
33.75158	-9.33156	906.48	905.8664
31.15054	-1.5319	1648.793	1647.722
34.68163	-1.83497	1616.797	1616.285
30.66942	-2.50666	1787.227	1787.94
31.36577	-2.66435	1438.365	1437.775
34.81976	-2.4366	1503.401	1503.994
35.54513	-2.06727	2023.758	2025.027
36.7041	-2.7426	1329.08	1331.327
30.70853	-3.59311	1480.568	1480.579
31.52459	-3.3357	1227.237	1226.476
32.40739	-3.40533	1260.648	1259.106
33.40612	-3.37028	1223.497	1222.609
34.30568	-3.51702	1195.581	1195.424
35.68594	-3.33609	1531.745	1533.076
36.7067	-3.43763	1252.592	1254.616
30.27451	-4.48061	1363.934	1364.365
31.33704	-5.04643	1086.121	1087.924
32.86178	-4.27797	1206.853	1205.608
33.44913	-4.53164	1269.622	1268.549
34.74014	-4.81388	1500.612	1501.313
35.77196	-4.89617	1398.76	1399.455
36.93538	-4.20501	1442.034	1445.133
37.91466	-4.5149	645.6495	646.8332
38.294	-4.80347	1377.01	1378.141
30.47756	-5.61465	1302.096	1303.41

31.6519	-5.32528	1095.001	1097.234
32.74324	-5.60968	1177.33	1176.329
33.15446	-5.3209	1212.944	1211.589
34.48965	-5.69791	1304.903	1305.276
35.96953	-5.9647	1068.264	1069.386
36.5778	-5.30954	1540.487	1542.904
37.28919	-5.5702	1265.28	1267.853
38.4851	-5.50057	396.81	397.0985
30.93963	-6.36465	1038.939	1041.106
31.2364	-6.29194	1212.957	1214.937
32.062	-6.72178	1182.605	1185.074
33.20577	-6.80421	1196.31	1197.356
34.96882	-6.35113	1147.857	1148.841
35.33372	-6.42848	889.997	890.9304
36.40572	-6.44562	785.518	786.2209
38.38644	-6.33831	280.2865	280.3397
31.02036	-7.49151	1564.35	1568.07
32.48452	-7.8553	1172.618	1172.54
33.35186	-7.83267	1466.519	1467.822
35.08183	-7.82931	963.954	967.1359
36.42055	-7.54399	568.112	569.0493
37.60958	-7.49352	177.942	178.2296
38.75919	-7.27636	454.128	454.2454
39.19347	-7.65947	144.337	143.4293
31.49291	-8.6802	1626.122	1628.173
32.7711	-8.87183	1556.828	1558.154
33.43946	-8.55656	1545.753	1546.877
34.38006	-8.74177	1098.162	1099.627
35.34904	-8.52257	2061.026	2064.443
36.42601	-8.67373	349.858	351.5394
37.0363	-7.80338	270.565	271.1516
38.88252	-8.81428	81.922	80.50555
39.52213	-8.92558	11.2	9.004566
33.87262	-9.60657	493.27	490.8104
34.58467	-9.59204	2197.029	2198.813
35.10255	-9.5468	1729.23	1732.451
35.89286	-10.0795	1031.176	1031.177
37.59638	-9.68195	689.517	688.0958
38.36225	-9.42253	386.268	384.9256
39.54433	-9.66848	146.327	144.4533
35.41951	-10.6284	1003.88	1005.632
36.12774	-10.489	860.407	860.4319
37.97549	-10.5414	472.636	470.7339
38.79549	-10.7384	425.343	423.7256
39.36419	-10.3005	132.87	131.4211

35.42838	-11.5783	582.925	585.9137
36.276	-11.2115	737.617	737.4611
30.67341	-1.19956	1661.615	1660.087
30.9399	-1.03157	1248.665	1246.983
31.40536	-1.20339	1157.072	1155.776
31.81272	-1.21569	1226.891	1225.446
30.94681	-1.52583	1453.696	1452.615
31.72584	-1.60542	1328.907	1327.276
31.11257	-1.75122	1564.334	1563.66
31.65481	-1.85085	1290.425	1288.752
33.0899	-2.09021	1186.188	1184.766
33.44979	-2.14508	1154.46	1153.333
33.86028	-1.99607	1243.462	1242.162
33.92437	-1.67785	1365.438	1364.201
34.03891	-1.17501	1196.976	1196.15
34.37179	-1.35104	1423.646	1423.275
34.12577	-1.45381	1244.15	1243.158
34.54423	-1.43692	1328.838	1328.533
34.23415	-1.73012	1292.478	1291.458
34.03152	-1.90236	1423.506	1422.258
34.34827	-1.44217	1195.081	1194.463
34.40243	-1.78965	1411.692	1410.862
30.85775	-2.48837	1569.69	1570.235
30.51495	-2.59559	1660.933	1661.73
30.72399	-2.79511	1527.738	1528.398
30.93224	-2.63267	1340.63	1341.115
31.44522	-2.13703	1227.252	1226.052
31.57876	-2.11068	1152.39	1150.848
31.68373	-2.38736	1176.852	1175.226
31.73461	-2.63552	1205.32	1203.832
31.00798	-2.77864	1310.178	1310.578
31.2005	-2.90516	1351.62	1351.544
31.47937	-2.79878	1350.878	1350.055
31.91406	-3.01033	1280.691	1279.336
32.41054	-2.45076	1162.099	1160.459
32.09344	-2.55839	1183.625	1181.917
32.65344	-2.64512	1254.599	1253.152
32.73788	-2.53332	1161.218	1159.755
32.98991	-2.68583	1230.18	1229.003
32.26253	-2.88801	1259.332	1257.805
32.42978	-2.8408	1198.3	1196.798
32.84948	-2.91554	1216.837	1215.618
33.09645	-2.84621	1175.848	1174.863
33.4589	-2.59694	1150.132	1149.427
33.33938	-2.96959	1223.235	1222.636

33.99719	-2.78155	1285.504	1285.518
33.86231	-2.21405	1139.654	1138.492
34.23937	-2.7779	1446.564	1446.695
34.14441	-2.16951	1193.173	1192.073
34.33061	-1.97007	1253.869	1252.893
34.64016	-2.08431	1356.403	1356.078
34.90761	-2.65449	1669.021	1670.032
34.78	-2.7561	1629.782	1630.767
34.45849	-2.28073	1291.057	1290.547
34.17401	-2.39787	1283.147	1282.323
30.96949	-3.28315	1244.087	1244.172
30.6023	-3.50079	1317.156	1317.397
30.9042	-3.63774	1302.125	1302.017
30.60944	-3.8976	1350.559	1350.658
31.21624	-3.04006	1242.866	1242.744
31.77741	-3.03342	1248.672	1247.448
31.90071	-3.46297	1239.859	1238.738
31.42028	-3.29145	1217.822	1217.25
31.35106	-3.18261	1261.607	1261.184
32.2393	-3.11356	1318.58	1317.11
32.60614	-3.18629	1197.562	1196.075
33.01835	-3.06396	1246.779	1245.68
32.86672	-3.30859	1211.085	1209.658
32.9644	-3.89965	1178.679	1177.131
32.59076	-3.82185	1279.661	1278.103
32.43617	-3.76442	1236.069	1234.592
32.50148	-3.90751	1207.368	1205.927
33.25431	-3.17077	1178.217	1177.285
33.51978	-3.13848	1240.317	1239.914
33.79075	-3.18618	1331.426	1331.418
33.82534	-3.62385	1149.061	1148.461
33.51049	-3.60922	1173.617	1172.611
33.1943	-3.87108	1165.14	1163.701
33.70383	-3.86624	1120.538	1119.625
33.97402	-3.91728	1083.894	1083.316
34.11678	-3.41978	1205.727	1205.774
34.44766	-3.53956	1220.344	1220.146
34.8137	-3.38377	1620.697	1621.001
34.20074	-3.03326	1369.822	1370.394
34.74927	-3.01277	1672.692	1673.826
34.21055	-3.85087	1077.933	1077.257
34.30768	-3.94793	1045	1044.303
34.51959	-3.89837	1044.34	1043.68
35.24544	-1.8558	1743.794	1744.686
35.15516	-2.00952	1736.031	1736.891

35.50245	-2.57946	1587.739	1588.88
35.13773	-2.90913	1624.325	1625.783
36.00489	-3.0017	831.9054	833.4755
35.87851	-2.61034	651.163	651.7327
35.69711	-2.16577	1328.406	1329.053
35.88485	-2.13596	1217.398	1217.372
35.50807	-2.37689	1879.26	1880.312
35.2707	-3.22133	1821.893	1823.13
35.8969	-3.38831	980.232	981.3684
35.34191	-3.51472	1050.84	1051.287
35.69109	-3.02932	2633.816	2635.694
35.45792	-3.2082	2486.186	2487.691
35.67328	-3.44252	1401.784	1402.748
35.55095	-3.85984	1754.231	1754.529
35.53336	-3.70743	1940.24	1940.478
35.7461	-3.66918	965.63	966.0956
35.92916	-3.70463	1021.187	1021.694
37.12536	-2.86715	1692.229	1695.633
37.46699	-2.93393	1988.707	1991.611
36.7794	-2.55815	1318.515	1321.083
36.4823	-2.52575	1695.022	1696.147
36.69566	-3.03887	1403.726	1405.873
36.3003	-2.82225	1267.515	1268.415
36.11425	-2.72652	1188.88	1189.573
32.23586	-4.19926	1191.1	1190.427
32.52105	-4.00181	1283.545	1282.185
32.51447	-4.40013	1190.72	1189.503
32.68744	-4.53604	1220.15	1218.888
32.09052	-4.63463	1126.452	1126.576
32.83759	-4.73809	1159.845	1158.493
32.59054	-4.92036	1151.416	1150.104
32.30842	-4.95151	1129.818	1129.311
33.1315	-4.03102	1132.551	1131.196
33.20549	-4.22301	1232.374	1231.207
33.70756	-3.99646	1087.678	1086.811
33.88349	-4.30239	1076.611	1075.945
33.85948	-4.56296	1090.245	1089.423
33.23603	-4.76457	1246.117	1244.894
33.1022	-4.86166	1256.352	1255.03
33.16983	-4.452	1234.001	1232.878
34.38444	-4.26758	1566.799	1566.339
34.09748	-4.38718	1082.84	1082.316
34.52959	-4.41855	1527.581	1527.456
34.74834	-4.13563	1588.214	1588.07
34.84126	-4.3484	1545.555	1545.993

34.87091	-4.66617	1617.311	1618.12
34.63467	-4.55424	1378.822	1379.071
34.25896	-4.67935	1228.685	1228.258
35.02218	-4.19336	1738.825	1739.448
35.362	-4.06709	1938.064	1938.741
35.79069	-3.99361	1000.106	1000.603
35.71727	-4.21494	1436.978	1437.866
35.8338	-4.72579	1495.851	1496.727
35.3795	-4.52507	1730.599	1731.803
35.316	-4.95978	1253.215	1253.719
35.18092	-4.66139	1703.028	1704.128
32.07264	-5.05708	1115.476	1116.29
32.31973	-5.09875	1144.046	1143.698
32.62964	-5.09673	1157.252	1156.006
32.28092	-5.26226	1139.432	1139.489
32.69529	-5.3651	1172.926	1171.803
32.50542	-5.72686	1102.3	1101.997
32.61171	-5.91853	1096.756	1096.519
32.88862	-5.80193	1148.679	1147.742
33.13053	-5.12733	1273.96	1272.569
33.47589	-5.31046	1170.872	1169.667
33.837	-5.042	1048.907	1047.73
33.49725	-5.14324	1234.321	1233.028
32.98395	-5.54684	1273.163	1271.861
33.26291	-5.93029	1228.532	1227.73
33.90094	-5.97423	1517.458	1517.549
33.64785	-5.43405	1200.625	1199.661
34.04431	-5.15208	1060.597	1059.699
34.75485	-4.99981	1560.787	1561.573
34.93374	-5.26024	1383.511	1384.279
34.66468	-5.54892	1387.057	1387.578
34.8259	-5.76349	1254.883	1255.452
34.36631	-5.64027	1306.718	1306.84
34.39538	-5.29878	1232.727	1232.661
34.05567	-6.01545	1550.504	1550.853
35.02521	-5.04956	1256.071	1256.866
35.43593	-5.20466	1185.728	1185.898
35.80939	-5.08932	1275.127	1275.908
35.84751	-5.48011	1153.87	1154.966
35.07794	-5.32046	1225.304	1225.87
35.12523	-5.8784	850.335	850.7771
35.32485	-5.95932	844.309	844.8037
35.7044	-5.6403	1132.119	1132.867
35.0615	-6.14184	829.0281	829.7047
35.49143	-6.09556	938.96	939.7951

35.01292	-6.64452	1058.436	1059.799
35.3926	-6.899	919.468	920.3018
35.62154	-6.59741	994.418	995.2557
35.97639	-6.69055	738.194	738.5598
35.99063	-6.22183	1039.621	1040.456
35.74943	-6.32256	1128.099	1128.987
36.09931	-3.5545	1072.884	1073.655
36.45097	-3.31353	1462.339	1463.529
36.67884	-3.1544	1767.497	1769.519
36.81719	-3.16584	1591.812	1594.382
36.93613	-3.55214	924.9171	927.5388
36.72132	-3.83522	1112.85	1115.259
36.38957	-3.81535	1577.334	1578.772
36.60498	-3.88872	1413.177	1415.38
37.14238	-3.33448	963.244	966.405
37.01285	-3.14641	1371.314	1374.629
37.52625	-3.41374	804.3437	806.3821
37.58796	-3.65544	839.734	841.2495
37.13406	-4.08081	1179.289	1181.981
37.4867	-3.92354	662.291	663.9367
36.07751	-4.80246	1226.511	1227.789
36.72465	-4.65221	1034.266	1037.274
36.37648	-4.27206	1310	1311.98
37.72775	-4.09267	864.1102	865.612
37.19924	-4.46102	1366.883	1370.193
37.15782	-4.80852	995.801	999.1849
37.68536	-4.55761	620.749	622.5433
38.0129	-4.16082	613.704	614.9354
38.07864	-4.64481	465.561	466.483
38.43407	-4.40548	417.725	419.0472
39.11337	-4.83061	61.523	61.85156
38.90964	-4.5328	145.172	146.4589
38.72315	-4.76651	362.403	363.9237
38.57384	-4.90325	339.171	340.5181
38.30871	-4.9758	404.3344	405.4036
38.29796	-4.91282	453.411	454.4961
36.16526	-5.14867	1471.975	1473.835
36.42172	-5.6225	1437.911	1439.806
36.65235	-5.31424	1321.702	1324.219
36.16066	-5.57197	1288.418	1290.203
36.45126	-5.89198	1196.272	1197.779
36.7236	-5.92926	1453.272	1455.346
37.18501	-5.40059	1367.464	1370.297
37.51376	-5.39116	1015.443	1017.508
37.93618	-5.39132	722.572	723.3901

37.78028	-5.90147	444.0086	445.2473
37.32334	-5.7878	837.331	839.621
37.01837	-5.92402	1111.681	1114.009
38.44673	-5.16038	316.714	317.6114
38.8058	-5.17175	217.4897	217.7748
38.98826	-5.40721	70.81	70.03446
38.85408	-5.77921	4.861	4.247227
38.03011	-5.42875	704.5466	705.2418
38.29708	-5.77373	399.343	399.9061
38.58121	-5.86073	211.987	211.9286
38.65975	-5.57847	116.851	116.6912
36.41167	-6.19657	1014.869	1015.93
36.87271	-6.133	1249.97	1251.961
36.98068	-6.84762	487.208	487.4313
36.70245	-6.64935	677.67	678.4102
36.25675	-6.95735	748.8481	749.3082
36.09631	-6.61079	876.1351	876.577
36.47243	-6.33977	1025.297	1026.214
36.13778	-6.36009	878.084	878.7797
37.16333	-6.24617	761.146	762.8649
37.62527	-6.1331	374.719	376.0113
37.91769	-6.7276	398.121	398.9112
37.13473	-6.78351	437.3769	437.6176
37.40343	-6.93516	517.524	517.8861
37.80862	-6.95005	333.155	333.8493
37.1204	-6.4748	553.88	554.9077
37.84226	-6.06954	365.067	366.2151
38.2419	-6.08328	385.412	386.0624
38.91043	-6.4433	6.011714	5.497932
38.99366	-6.7459	138.622	138.343
38.32531	-6.63752	212.6252	212.5544
38.78925	-6.63012	82.548	82.03611
38.17213	-6.84002	161.1042	161.3137
39.0624	-6.91598	262.154	262.0687
38.77432	-6.04353	5.883	5.455926
38.93412	-7.72658	171.044	170.2016
38.76622	-7.89832	36.312	35.39976
38.32233	-7.30401	72.88821	72.63558
38.244	-7.7744	54.784	54.15066
38.6893	-7.43614	141.542	141.4491
38.50531	-7.13707	87.444	87.24304
38.12478	-7.66961	59.817	59.35103
35.59079	-7.84429	1544.519	1547.947
35.86338	-7.74893	1575.531	1578.312
35.77311	-7.58987	1359.164	1361.323

35.79795	-7.41985	1246.28	1247.646
35.49289	-7.35686	731.756	732.891
35.4222	-7.67198	987.9238	990.5375
35.98108	-7.10703	726.493	727.0344
35.7924	-7.95799	1853.619	1857.136
35.3204	-7.21791	882.134	883.1397
36.49044	-7.11039	1117.25	1117.764
36.12651	-7.47249	1497.546	1498.921
36.90858	-7.07072	550.6	550.8726
36.98352	-7.40592	509.975	510.495
36.97772	-7.66155	287.595	288.1778
36.65428	-7.5217	517.663	518.3692
36.74189	-7.33811	768.012	768.6476
36.12034	-7.65784	1290.471	1292.274
37.81622	-7.36756	137.396	137.5318
37.53719	-7.13426	1358.628	1359.083
37.78275	-7.10567	395.055	395.5707
37.76805	-7.53364	184.334	184.3446
37.18085	-7.34384	631.211	631.6195
37.26855	-7.10356	540.023	540.2351
39.17804	-7.15813	108.609	108.4247
39.06851	-7.35677	91.553	91.31912
39.33642	-7.39931	9.948142	9.280852
39.14787	-7.4923	69.33789	68.78652
39.53108	-7.08067	19.287	18.61281
38.79875	-8.55708	205.801	204.4246
38.82721	-8.93616	146.142	144.7916
38.79961	-8.3635	435.126	433.788
38.75994	-7.99975	60.574	59.5062
39.18239	-8.14012	4.923	3.451164
39.2827	-8.39494	8.538	6.964556
39.27379	-8.60804	25.876	24.26179
39.33915	-8.81773	100.7443	98.97911
39.02631	-8.78205	53.4008	51.8975
31.0789	-6.35852	1065.915	1068.002
31.1402	-6.60983	1009.541	1011.934
31.28349	-6.72372	978.73	981.3104
31.35222	-6.45137	1041.485	1043.653
31.72406	-6.50203	1200.322	1202.85
32.20361	-6.30436	1097.677	1099.308
32.48916	-6.04361	1090.202	1090.496
31.81395	-6.70251	1239.627	1242.23
32.71334	-6.35079	1107.393	1107.91
33.03308	-6.30034	1139.074	1139.091
32.16469	-6.83118	1125.135	1127.437

32.48808	-6.74394	1162.179	1163.935
30.57022	-7.05386	814.676	817.4309
30.65782	-7.4336	791.006	793.1568
31.13983	-7.11848	969.117	972.6997
31.0897	-7.34292	1551.699	1555.572
31.22864	-7.53648	1694.466	1699.057
31.35455	-7.74588	1921.268	1926.042
31.39159	-7.2532	925.851	929.641
31.47723	-7.57744	832.5801	837.2427
31.20958	-7.84774	1708.362	1712.46
31.67485	-7.33475	816.382	819.5365
33.56422	-7.92479	1372.789	1373.857
33.40266	-7.62299	1440.464	1441.76
33.43676	-7.42825	1333.311	1334.643
33.7554	-7.31149	1400.529	1402.023
33.48473	-7.14487	1288.288	1289.675
33.52629	-6.93685	1237.466	1238.775
33.36349	-6.82072	1204.149	1205.257
31.04923	-8.12321	1386.282	1388.177
31.20566	-8.46649	1200.736	1202.16
31.3817	-8.25536	1715.928	1719.263
31.67272	-8.13311	1907.065	1911.107
31.66881	-8.65791	1823.64	1826.259
31.77023	-8.86148	1563.504	1565.733
31.94559	-8.76895	1499.803	1502.093
31.83676	-8.35448	1613.918	1616.945
31.97966	-8.26216	866.0275	868.0902
32.06217	-8.57776	1573.928	1575.844
32.13229	-8.93019	1459.807	1461.481
32.27673	-8.84116	1394.924	1396.363
32.32968	-8.30513	817.993	817.7589
32.47942	-8.44816	870.82	870.4772
32.60698	-8.7412	1308.315	1309.179
32.75271	-8.52993	829.024	829.1143
33.00076	-8.39192	1037.266	1037.906
32.7905	-7.81838	1190.354	1191.084
32.68438	-8.06568	1077.949	1077.571
32.88364	-9.15374	1529.36	1531.061
32.7901	-9.2941	1562.952	1564.387
32.50041	-9.0863	1545.13	1546.437
29.76761	-4.44072	1716.011	1715.915
29.67317	-4.76577	1006.005	1005.593
30.0019	-4.98273	1090.368	1090.62
29.74197	-4.8826	826.419	826.0776
30.12029	-4.15934	1216.356	1217.313

30.10137	-4.5606	1293.28	1293.597
30.0131	-4.81145	1223.866	1224.05
30.20852	-4.78583	1102.188	1102.754
30.42043	-4.28279	1153.917	1154.126
30.48749	-4.20215	1226.028	1226.122
30.5805	-4.58121	1106.487	1106.965
30.26337	-4.06294	1223.673	1224.562
30.85261	-4.90757	1061.437	1062.428
29.83242	-5.1902	782.934	782.7392
29.84585	-5.55717	870.206	870.2109
29.95847	-5.8132	778.759	779.5506
29.86046	-5.97148	776.045	777.5323
30.38079	-5.10188	993.865	994.8191
30.76563	-5.10488	1123.43	1124.679
30.37434	-5.26215	1391.619	1392.552
30.59591	-5.62864	1307.827	1309.388
30.53305	-5.47262	1678.033	1679.316
30.8621	-5.85734	1174.424	1176.444
30.73852	-5.98663	1333.264	1335.338
31.03647	-5.10862	1072.812	1074.181
31.63213	-4.93297	1118.21	1120.101
31.79772	-5.06017	1081.175	1083.053
31.60341	-5.4765	1107.298	1109.525
31.49895	-5.50458	1065.187	1067.456
31.1297	-6.06235	1156.376	1158.317
31.28215	-5.66772	1121.855	1123.894
29.73934	-6.16515	772.079	774.5321
30.01252	-6.47599	773.531	776.4454
30.43517	-6.81135	775.952	778.7357
30.74562	-6.49612	1072.157	1074.556
30.70957	-6.32184	1098.111	1100.407
30.32406	-6.20456	1838.644	1840.793
30.93428	-6.08663	1320.538	1322.577
33.25817	-8.03043	1328.394	1329.708
33.65782	-8.43412	1457.094	1457.85
33.16192	-8.41324	1202.984	1203.965
33.27436	-8.71451	1022.77	1024.075
33.03329	-8.61917	889.875	890.9354
33.45141	-8.89717	1689.788	1690.992
33.83782	-8.81803	1193.639	1194.528
33.13139	-8.96796	1673.774	1675.478
34.21742	-8.80738	1113.725	1115.027
34.61078	-8.91435	1465.831	1468.543
34.80478	-8.83857	1646.333	1649.326
34.95634	-8.61294	1718.138	1721.175

34.49978	-8.55657	1045.474	1046.75
34.84343	-8.21424	1071.862	1074.746
35.0352	-8.24488	1560.853	1564.469
35.28869	-8.74039	1277.831	1280.752
35.31146	-8.2648	1888.401	1892.57
35.88026	-8.23605	1971.417	1974.462
35.58074	-8.49778	1755.136	1758.156
35.02865	-8.83263	1496.029	1499.264
35.47525	-8.05607	1796.959	1801.092
32.95525	-9.13017	1624.097	1625.871
33.41835	-9.07013	2037.582	2038.706
33.17777	-9.37126	1601.301	1602.241
33.77281	-9.33088	769.572	768.9835
33.90078	-9.09241	2744.082	2744.82
33.55544	-9.28716	1215.774	1215.853
34.21675	-9.45396	2119.821	2119.701
34.09924	-9.25916	2277.163	2277.899
34.41277	-9.30776	2294.583	2296.753
34.78467	-9.36284	1956.569	1960.419
34.78467	-9.10803	1846.481	1850.202
34.53661	-9.7674	1789.101	1789.249
34.79971	-9.85546	1379.558	1381.017
35.24202	-9.27875	1644.969	1647.945
35.25916	-9.63811	1533.796	1536.084
35.37382	-9.86939	1282.76	1283.869
35.61695	-9.95978	954.197	954.384
37.7581	-9.14687	377.696	376.7496
37.91801	-9.80522	511.603	510.008
35.31497	-10.4757	1080.47	1081.754
34.67749	-10.1046	1384.228	1383.241
34.9367	-10.128	1337.48	1338.115
35.65137	-10.1132	924.866	925.1125
35.67038	-10.3859	1040.599	1041.314
35.65633	-10.6747	1131.25	1132.724
35.87945	-10.5542	1010.817	1011.391
35.48873	-10.9055	931.193	933.7669
34.99216	-10.9487	1341.747	1344.027
35.19014	-10.7166	946.929	948.8482
34.68242	-10.8198	483.78	483.3791
34.90666	-10.5378	949.389	949.3762
34.59613	-10.4767	501.634	499.4908
36.13696	-10.2912	778.292	778.3697
36.32382	-10.2977	835.762	835.6636
36.5239	-10.1908	868.775	868.4389
36.73392	-10.2207	711.4411	710.5871

36.95256	-10.7555	822.2304	820.8252
36.52189	-10.7631	964.784	964.0265
36.09638	-10.9254	808.055	808.3492
36.68543	-10.7976	878.828	877.8003
37.79808	-10.0852	598.35	596.391
37.45111	-10.8687	516.881	515.1992
34.64782	-11.1035	511.457	512.0099
34.91259	-11.0961	1611.432	1613.53
34.9597	-11.5065	493.3244	495.7842
35.23101	-11.4022	1063.437	1066.846
35.17395	-11.1251	973.121	976.2692
35.45099	-11.2443	757.48	760.636
35.63049	-11.4754	621.0847	623.7739
35.40231	-11.388	637.567	640.8197
36.16569	-11.3302	716.642	716.9299
36.03979	-11.0506	636.47	636.9815
36.65913	-11.4789	597.001	596.0321
36.8609	-11.3205	724.181	722.9579
36.48409	-11.14	606.11	605.2854
37.57924	-11.0258	447.464	446.0504
37.80082	-10.8989	404.263	402.4662
37.08538	-11.5883	462.021	460.9808
38.47947	-10.1228	269.969	268.5739
38.12968	-10.63	491.991	490.2537
38.93747	-10.231	448.962	447.568
38.75797	-10.3612	444.022	442.6105
38.24055	-10.3682	375.369	373.8648
38.23857	-10.8969	334.94	333.1383
38.51793	-10.9146	304.869	303.0901
38.45496	-11.1992	301.667	299.5797
38.947	-11.0329	242.108	240.1701
38.21476	-9.13611	270.215	268.9946
38.70277	-9.33565	278.346	277.1001
38.68537	-9.17374	278.1435	276.8834
38.01534	-9.70092	426.949	425.4403
38.31066	-9.93914	350.016	348.5333
38.50967	-9.7886	322.929	321.5671
39.71649	-10.0039	3.367	1.568546
39.26629	-10.9592	733.382	731.5124
39.02614	-10.4948	299.494	298.0227
39.33725	-10.6489	466.005	464.3107
39.43359	-10.8571	495.289	493.3213
39.81127	-10.6859	245.829	243.7991
39.66813	-10.1698	56.481	54.79199
39.77881	-10.3547	92.002	90.18567

40.05429	-10.5068	162.012	160.3772
40.34638	-10.4993	8.923	8.118876
39.27339	-10.1468	685.124	683.7911
39.10806	-9.66703	102.829	101.4181
39.12533	-9.90845	329.969	328.548
39.40785	-9.29212	161.313	159.4482
39.56303	-9.1194	17.34	15.03141
39.31566	-9.06	38.624	36.95757
39.05269	-9.11223	164.1039	162.689
38.99424	-9.43545	201.205	199.8128